Supporting Information

[$RuCl_2(\eta^6$-*p*-cymene)] complexes bearing phosphinous acid ligands: preparation, application in C-H bond functionalization and mechanistic investigations

Lionel V. Graux,[a] Michel Giorgi,[b] Gérard Buono[a] and Hervé Clavier[a*]

[a] Aix Marseille Université, Centrale Marseille, CNRS, iSm2 UMR 7313, 13397, Marseille, France.

[b] Aix Marseille Université Spectropole, Fédération des Sciences Chimiques de Marseille, 13397 Marseille, France.

E-mail: herve.clavier@univ-amu.fr

I. General considerations

All reagents were obtained from commercial sources and used as received. Secondary phosphine oxides **4c** and **4e-g** were obtained from chemical suppliers. Other SPOs were prepared according to literature procedures: **4b**[1], **4d**[1], **4h**,[2] **4i**,[2] **4j**,[3] **4k**[4] and **4l**.[2] Solvents (THF, DCM, toluene and Et_2O) were purified and dried over Braun solvent purification system (MB-SPS-800) or dried by standard procedures prior to use.[5] Analytical Thin Layer Chromatography (TLC) was carried out on Merck silica gel60 F_{254}. Products were revealed by ultraviolet light (254 or 366 nm) and stained with dyeing reagents solutions as 5% phosphomolybdic acid solution, potassium permanganate solution or *p*-anisaldehyde solution in ethanol followed by gentle heating. Flash chromatography was performed on Combiflash® Companion or with Merck silica gel 60 (230-400 mesh). ^1H, ^{13}C, ^{31}P and ^{19}F NMR spectra were recorded in $CDCl_3$ at ambient temperature on Bruker Avance III 300 or 400 spectrometers operating at 300 and 400 MHz respectively for ^1H. ^{13}C, ^{31}P and ^{19}F nuclei were observed with ^1H decoupling. Solvent residual signals were used as internal standard.[6] Chemical shifts (δ) and coupling constants (*J*) are given in ppm and Hz respectively. The peaks patterns are indicated as the following format multiplicity (s: singlet; d: doublet; t: triplet; q: quartet; sept: septuplet; m: multiplet; dd: doublet of doublet; dt: doublet of triplet; dm: doublet of multiplet, etc.). The prefix br. indicates a broadened signal. HRMS were recorded on SYNAPT G2 HDMS (Waters) or on QStar Elite (Applied Biosystems SGIEX) equipped with an Atmospheric Pressure Ionization (API) source. Mass spectra were obtained a Time Of Flight (TOF) analyser. X-ray Diffraction: Intensity data were collected on a Brucker-Nonius KappaCCD diffractometer using MoKα radiation (0.71073 Å) at 293(2) K. Data reduction was performed using the HKL-2000 software package. The structure was resolved using the software SIR92[7] by the direct methods and refined using SHELXL-97.[8] For compound **5d,** intensity data were collected on a Agilent SuperNova AtlasS2 diffractometer using MoKα radiation (0.71073 Å) at 293(2) K. Data reduction was performed using the CrysAlisPro software package (version 1.171.37.31). The structure was resolved using the software SHELXS-97 by the direct methods and refined using SHELXL-2013-4. The CIF files of compounds have been deposited with CCDC numbers:

Compound **5b**: 1434226
Compound **5c**: 1434227
Compound **5d**: 1434228
Compound **5h**: 1434229
Compound **5i**: 1434230
Compound **5k**: 1434231
Compound **5l**: 1434232

II. Preparation of Complexes [$RuCl_2(\eta^6$-*p*-cymene)(PR_3)]

[$RuCl_2(\eta^6$-*p*-cymene)(PPh_3)][9]

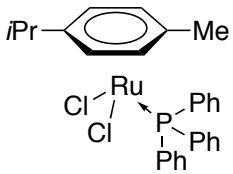

According to the general procedure, the compound was prepared from PPh_3. The complex was obtained as a deep-red solid (106 mg, 94%). ^{1}H NMR (400 MHz, $CDCl_3$): δ (ppm) = 7.90-7.75 (m, 6H, H^{Ar}), 7.40-7.25 (m, 9H, H^{Ar}), 5.18 (d, *J*(H,H) = 5.9 Hz, 2H, H^{Ar}), 4.99 (d, *J*(H,H) = 5.9 Hz, 2H, H^{Ar}), 2.82 (sept, *J*(H,H) = 7.0 Hz, 1H, C*H*(CH_3)$_2$), 1.85 (s, 3H, C-C*H*$_3$), 1.08 (d, *J*(H,H) = 7.0 Hz, 6H, CH(C*H*$_3$)$_2$). ^{13}C NMR (101 MHz, $CDCl_3$): δ (ppm) = 134.3 (C^{Ar}-H), 133.7 (C^{Ar}-P), 130.2 (C^{Ar}-H), 127.9 (C^{Ar}-H), 111.2 (C^{Ar}), 96.0 (C^{Ar}), 89.1 (C^{Ar}-H), 87.2 (C^{Ar}-H), 30.2 (CH), 22.0 (CH_3), 17.8 (CH_3). ^{31}P{^{1}H} NMR (162 MHz, $CDCl_3$): δ (ppm) = 24.2 (s).

Complex [$RuCl_2(\eta^6$-*p*-cymene)(PCy_3)][9]

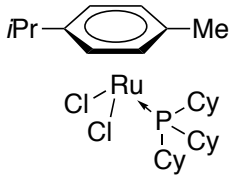

According to the general procedure, the compound was prepared from PCy_3. The complex was obtained as a deep-red solid (108 mg, 84%). ^{1}H NMR (400 MHz, $CDCl_3$): δ (ppm) = 5.56 (m, 4H, H^{Ar}), 2.84 (sept, *J*(H,H) = 6.9 Hz, 1H, C*H*(CH_3)$_2$), 2.41 (m, 3H, C*H*), 2.20-1.10 (m, 30H, C*H*$_2$), 2.09 (s, 3H, C-C*H*$_3$), 1.29 (d, *J*(H,H) = 6.9 Hz, 6H, CH(C*H*$_3$)$_2$). ^{13}C NMR (101 MHz, $CDCl_3$): δ (ppm) = 106.7 (C^{Ar}), 94.2 (C^{Ar}), 88.2 (C^{Ar}-H), 83.6 (C^{Ar}-H), 35.7 (CH), 30.4 (CH_2), 29.5 (CH_2), 27.4 (CH_2), 26.3 (CH), 22.3 (CH_3), 17.7 (CH_3). ^{31}P{^{1}H} NMR (162 MHz, $CDCl_3$): δ (ppm) = 25.3 (s).

Complex [$RuCl_2(\eta^6$-*p*-cymene)(P{OPh}$_3$)][10]

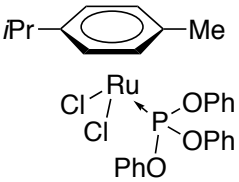

According to the general procedure, the compound was prepared from $P(OPh)_3$. The complex was obtained as a deep-red solid (109 mg, 89%). ^{1}H NMR (400 MHz, $CDCl_3$): δ (ppm) = 7.35-7.20 (m, 12H, H^{Ar}), 7.20-7.10 (m, 3H, H^{Ar}), 5.41 (d, *J*(H,H) = 6.0 Hz, 2H, H^{Ar}), 5.09 (d, *J*(H,H) = 6.0 Hz, 2H, H^{Ar}), 2.70 (sept, *J*(H,H) = 6.9 Hz, 1H, C*H*(CH_3)$_2$), 1.81 (s, 3H, C-C*H*$_3$), 1.18 (d, *J*(H,H) = 6.9 Hz, 6H, CH(C*H*$_3$)$_2$). ^{13}C NMR (101 MHz, $CDCl_3$): δ (ppm) = 151.5 (C^{Ar}), 129.4 (C^{Ar}-H), 125.1 (C^{Ar}-H), 121.7 (C^{Ar}-H), 109.4 (C^{Ar}), 103.1 (C^{Ar}), 88.9 (C^{Ar}-H), 88.6 (C^{Ar}-H), 30.6 (CH), 22.1 (CH_3), 18.0 (CH_3). ^{31}P{^{1}H} NMR (162 MHz, $CDCl_3$): δ (ppm) = 105.0 (s).

III. Discussion on ^{1}H NMR of complexes [$RuCl_2(\eta^6$-*p*-cymene)(PA)] 5

In ^{1}H NMR, it is worthwhile to note the effect of the ligand PA bound to the ruthenium on the aromatic and the methyl- and isopropyl-protons of the *p*-cymene moiety. With symmetrical phosphinous acids (**4b-4e**), the protons pairs H^2,H^6 and H^3,H^5 were isochronous and showed two doublets, the equivalent methyl group Me^8,Me^9 appeared as un singlet. With a dissymmetrical PA ligand, presenting a stereogenic phosphorus atom in the coordination sphere, the four CH aromatic carbons were anisochronous appeared as four doublets and the two methyl groups of the isopropyl substituent of the *p*-cymene showed two doublets (Fig. 1).

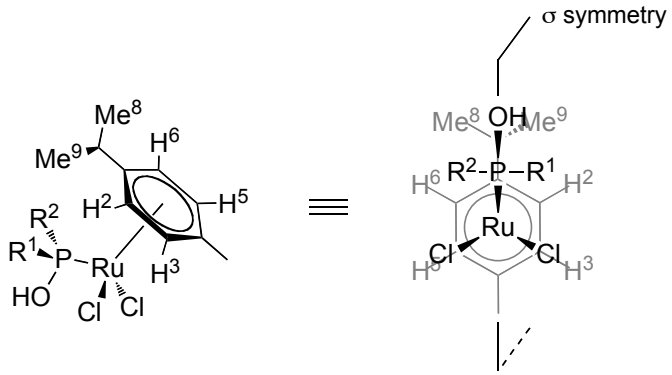

Fig 1. Representation of [$RuCl_2(\eta^6$-*p*-cymene)(PA)] complexes

A NOESY (Nuclear Overhauser Effect Spectroscopy) study realized on complexes **5k** and **5l** revealed a correlation between the two methyl groups of the *p*-cymene isopropyl substituents with the *ortho* protons H^2 and H^6 and the *p*-cymene methyl with H^3 and H^5. Besides, the substituent R (*tert*-butyl or cyclohexyl) of the phosphinous acid was correlated with one of the *ortho* hydrogen H^3 or H^5.

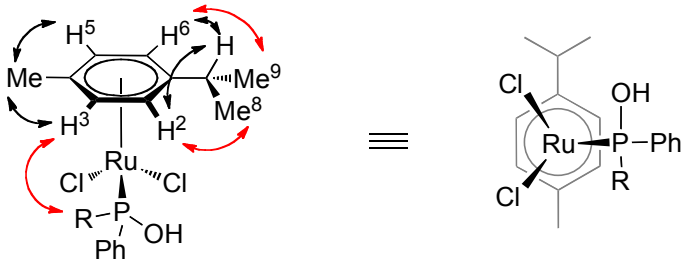

Fig. 2 Ruthenium complexes **5k** (R = Cy) and **5l** (R = *t*Bu): NOESY study

IV. Percent of buried volumes of various ligands L and η^6-*p*-cymene in [$RuCl_2(\eta^6$-*p*-cymene)(L)]

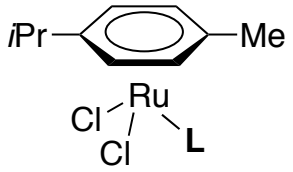

Entry	L	d(Ru-L) (Å)	$\%V_{bur}$(L)	d(Ru-C_{avg}) (Å)	$\%V_{bur}(\eta^6$-*p*-cymene)	Reference
1	Me_2POH	2.3078(10)	21.9	2.212(3)	48.0	[11]
2	Cy_2POH	2.3376(9)	24.4	2.215(4)	47.3	This work
3	Ph_2POH	2.3120(8)	24.6	2.216(3)	47.0	This work
4	$(p\text{-F-}C_6H_4)_2POH$	2.3009(8	24.6	2.212(3)	47.5	This work
5	MePhPOH	2.3130(6)	22.7	2.210(3)	47.3	This work
6	*n*BuPhPOH	2.3017(10)	22.7	2.209(4)	48.4	This work
7	CyPhPOH	2.3342(8)	24.1	2.212(3)	47.5	This work
8	*t*BuPhPOH	2.3680(7)	24.4	2.214(3)	47.9	This work
9	Ph_2PH	2.313(2)	23.2	2.209(7)	47.4	[12]
10	Ph_2PCH_2OH	2.3516(8)	25.1	2.217(3)	47.6	[13]
11	Ph_2P*n*Bu	2.352(2)	25.6	2.211(8)	47.4	[14]
12	PPh_3	2.3438(6)	26.8	2.218(2)	47.6	[15]
13	$P(OPh)_3$	2.2642(8)	24.7	2.214(3)	48.0	[16]
14	P(*m*-Tol)$_3$	2.374(2)	26.9	2.214(6)	47.5	[17]
15	PBn_3	2.359(1)	24.5	2.216(2)	47.4	[18]
16	$PCyp_3$	2.3878(10)	26.2	2.204(4)	47.4	[19]
17	PCy_3	2.387(2)	27.0	2.204(2)	47.0	[17]
18	$P(NC_4H_4)_3$	2.282(2)	27.4	2.227(2)	47.2	[18]
19	PhP(*i*Pr)biphenyl	2.4258(19)	27.8	2.214(8)	46.9	[20]
20	*i*BuPhoban	2.3895(7)	26.0	2.213(3)	47.5	[19]
21	IMes	2.142(4)	27.9	2.219(5)	47.0	[21]
22	ICy	2.093(3)	24.7	2.210(3)	47.6	[22]
23	IiPr	2.0828(14)	24.9	2.2177(15)	47.7	[23]
24	$SICH_2$-*o*-Tol	2.021(13)	25.8	2.186(14)	47.7	[24]

Parameters used for Samb*V*ca calculations: 3.50 Å was selected as the value for the sphere radius, exact distances between the ligand and the metal were considered, usually irrelevant in crystallography hydrogen atoms were omitted and Bondi radii scaled by 1.17 were used as recommended by Cavallo.

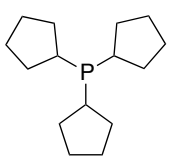

$PCyp_3$

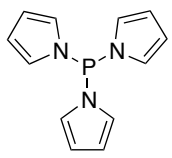

$P(NC_4H_4)_3$

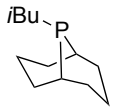

***i*BuPhoban**

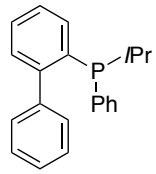

PhP(*i*Pr)biphenyl

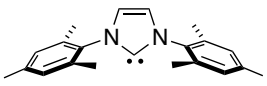

IMes

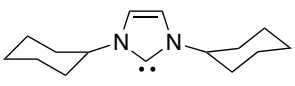

ICy

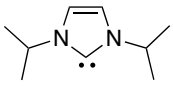

I*i*Pr

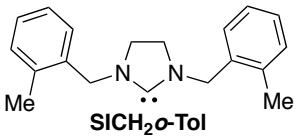

$SICH_2$*o*-Tol

V. Percent of buried volumes of phosphinous acid *t*Bu$_2$POH

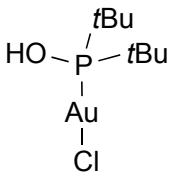

%V_{bur} (*t*Bu$_2$POH) = 32.6[25]

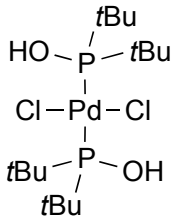

%V_{bur} (*t*Bu$_2$POH) = 29.1[26]

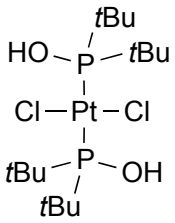

%V_{bur} (*t*Bu$_2$POH) = 29.7[27]

Percent of buried volumes of phosphinous acids calculated from phosphinito-phosphinous acid complexes led to an overestimation of the value.

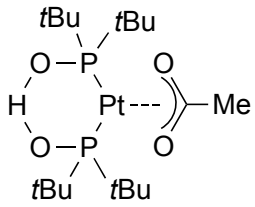

%V_{bur} (*t*Bu$_2$POH) = 32.7[28]

VI. Percent of buried volumes of phosphinous acid Ad$_2$POH

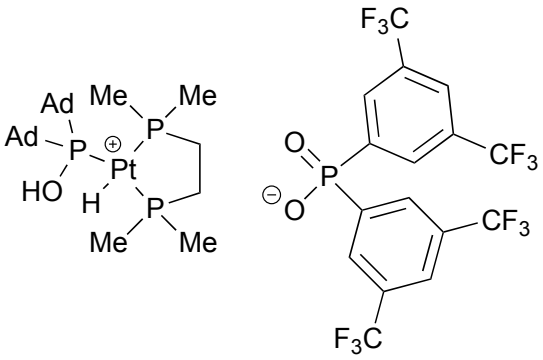

%V_{bur} (Ad$_2$POH) = 31.4[29]

Percent of buried volumes of phosphinous acids calculated from phosphinito-phosphinous acid complexes led to an overestimation of the value.

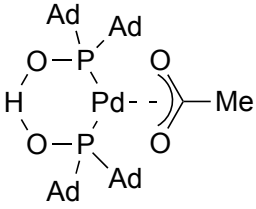

%V_{bur} (Ad$_2$POH) = 33.1[30]

VII. C-H activation of 2-phenylpyridine[31]

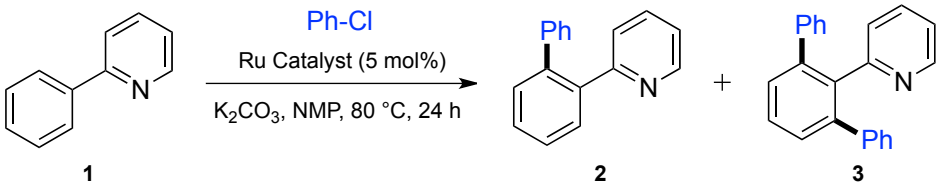

General procedure: 2-phenylpyridine **1** (155.2 mg, 142 µL, 1 mmol), chlorobenzene (2.2 mmol, 2.2 equiv.), K_2CO_3 (415 mg, 3 mmol, 3 equiv.) and ruthenium(II) complex (5 mol %) were solubilized in dry NMP (2 mL). The mixture was stirred at 80 °C for 24 h. The reaction mixture was then cooled and dissolved in water (75 mL). Aqueous layer was extracted with EtOAc (50 mL). Organic phase was washed with water (2x50 mL). The combined aqueous phases were back extracted with EtOAc (50 mL). The combined organic phases were washed with brine, dried over $MgSO_4$ and concentrated under vacuum. The residue was purified by silica gel flash chromatography (PE/AcOEt 9:1) to afford a mixture of 2-biphenyl-2'-pyridine **2** and 2-terphenyl-2'-pyridine **3**.

2-biphenyl-2'-pyridine **2**

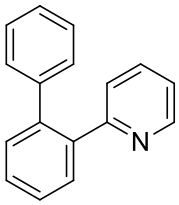

The ^1H and ^{13}C NMR spectrum of **2** were obtained from a mixture 9:1 of **2** and **3**. ^1H NMR (300 MHz, $CDCl_3$): δ (ppm) = 8.68 (ddd, *J*(H,H) = 4.8, 1.7 and 1.0 Hz, 1H, N-C*H*^{Ar}), 7.80-7.70 (m, 1H, *H*^{Ar}), 7.55-7.45 (m, 3H, *H*^{Ar}), 7.41 (td, *J*(H,H) = 7.7 Hz and 1.8 Hz, 1H, *H*^{Ar}), 7.30-7.10 (m, 6H, *H*^{Ar}), 6.93 (td, *J*(H,H) = 7.7 and 1.8 Hz, 1H, H^{Ar}). ^{13}C NMR (75 MHz, $CDCl_3$): δ (ppm) = 159.2 (C^{Ar}-N), 149.4 (N-*C*^{Ar}-H), 141.3 (C^{Ar}), 140.6 (C^{Ar}-H), 139.5 (C^{Ar}), 135.1 (C^{Ar}), 130.4 (C^{Ar}-H), 129.7 (C^{Ar}-H), 128.5 (C^{Ar}-H), 128.0 (C^{Ar}-H), 127.6 (C^{Ar}-H), 126.6 (C^{Ar}-H), 125.3 (C^{Ar}-H), 121.2 (C^{Ar}-H).

2-terphenyl-2'-pyridine **3**

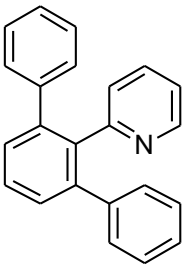

^1H NMR (300 MHz, $CDCl_3$): δ (ppm) = 8.31 (ddd, *J*(H,H) = 4.8, 1.7 and 0.9 Hz, 1H, N-C*H*^{Ar}), 7.55-7.40 (m, 3H, *H*^{Ar}), 7.30 (td, *J*(H,H) = 7.7 and 1.8 Hz, 1H, *H*^{Ar}), 7.20-7.05 (m, 10H, *H*^{Ar}), 6.95-6.85 (m, 2H, *H*^{Ar}). ^{13}C NMR (75 MHz, $CDCl_3$): δ (ppm) = 158.9 (C^{Ar}-N), 148.5 (N-*C*^{Ar}-H), 141.9 (C^{Ar}), 141.6 (C^{Ar}-H), 138.5 (C^{Ar}), 134.9 (C^{Ar}), 129.5 (C^{Ar}-H), 129.5 (C^{Ar}-H), 128.2 (C^{Ar}-H), 127.7 (C^{Ar}-H), 126.8 (C^{Ar}-H), 126.3 (C^{Ar}-H), 120.9 (C^{Ar}-H).

VIII. Additional results in catalysis

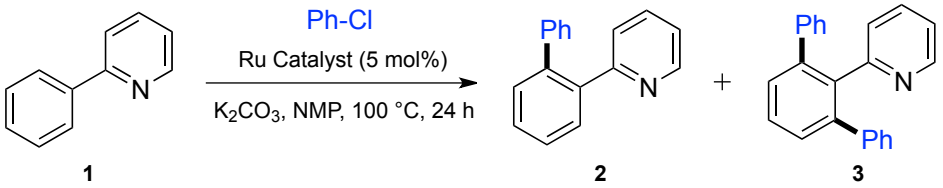

Entry	Catalyst	Additive	Yield (%)	
			2	3
1	$[RuCl_2(p\text{-cymene})]_2$		8	2
2	$[RuCl_2(p\text{-cymene})]_2$	$Ad_2P(O)H$ **4f** (5 mol%)	0	80
3	$[RuCl_2(p\text{-cymene})]_2$	$Ad_2P(O)H$ **4f** (10 mol%)	0	83
4	$[RuCl_2(p\text{-cymene})]_2$	PhCyP(O)H **4k** (5 mol%)	0	82
5	$[RuCl_2(p\text{-cymene})]_2$	PhCyP(O)H **4k** (10 mol%)	36	54
6	$[RuCl_2(\eta^6\text{-}p\text{-cymene})(CyPhPOH)]$ **5k**		0	84
7	$[RuCl_2(\eta^6\text{-}p\text{-cymene})(CyPhPOH)]$ **5k**	PhCyP(O)H **4k** (5 mol%)	6	81

[a] Reaction conditions: 2-phenylpyridine **1** (142 µL, 1 mmol), chlorobenzene (243 µL, 2.2 mmol, 2.2 equiv), K_2CO_3 (415 mg, 3 mmol, 3 equiv.), 5 mol% of Ru complex (2.5 mol% for $[RuCl_2(p\text{-cymene})]_2$), NMP (2 mL), 100 °C, 24 h.

IX. Preparation of $[RuX_2(\eta^6\text{-}p\text{-cymene})]_2$[32]

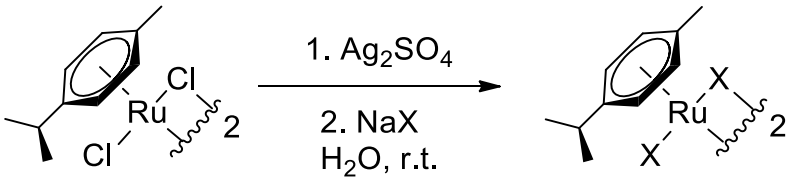

General Procedure: To a red suspension of $[RuCl_2(\eta^6\text{-}p\text{-cymene})]_2$ (100 mg, 0.16 mmol) in water (20 mL), silver nitrate (102 mg, 0.33 mmol) was added. The reaction mixture was stirred at room temperature for 2 hours. After filtration, NaBr (168 mg, 1.63 mmol) or NaI (245 mg, 1.63 mmol) was added to the yellow solution. The red precipitate was filtered and washed with water (3 x 5mL). The deep-red solid was solubilized in DCM, dried over $MgSO_4$, filtered off and dried under vacuum. Recrystallization from $CHCl_3$/toluene gave crystals of desired product.

Complex $[RuBr_2(\eta^6\text{-}p\text{-cymene})]_2$

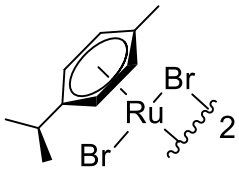

According to general procedure, the expected complex was obtained as brown crystals (56 mg, 44 %). ^{1}H NMR (300 MHz, $CDCl_3$): δ (ppm) = 5.48 (d, *J*(H,H) = 6.0 Hz, 2H, H^{Ar}), 5.36 (d, *J*(H,H) = 6.0 Hz, 2H, H^{Ar}), 2.94 (sept, *J*(H,H) = 7.0 Hz, 1H, $CH(CH_3)_2$), 2.20 (s, 3H, C-CH_3), 1.26

(d, *J*(H,H) = 6.9 Hz, 6H, CH(C*H*$_3$)$_2$). ^{13}C NMR (101 MHz, $CDCl_3$): δ (ppm) = 102.3 (C), 96.9 (C), 81.5 (C^{Ar}-H), 81.3 (C^{Ar}-H), 31.0 (CH), 22.4 (2 CH_3), 19.5 (CH_3).

Complex [RuI$_2$(η^6-*p*-cymene)]$_2$

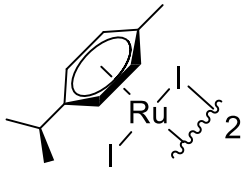

According to general procedure, the expected complex was obtained as dark-red crystals (149 mg, 95 %). ^{1}H NMR (300 MHz, $CDCl_3$): δ (ppm) = 5.54 (d, *J*(H,H) = 5.9 Hz, 2H, *H*^{Ar}), 5.43 (d, *J*(H,H) = 5.9 Hz, 2H, *H*^{Ar}), 3.02 (sept, *J*(H,H) = 7.0 Hz, 1H, C*H*(CH_3)$_2$), 2.36 (s, 3H, C-CH_3), 1.25 (d, *J*(H,H) = 6.9 Hz, 6H, CH(C*H*$_3$)$_2$). ^{13}C NMR (101 MHz, $CDCl_3$): δ (ppm) = 104.5 (C), 97.7 (C), 82.7 (C^{Ar}-H), 82.2 (C^{Ar}-H), 31.6 (CH), 22.9 (2 CH_3), 20.4 (CH_3).

X. Synthesis of intermediate 8[33]

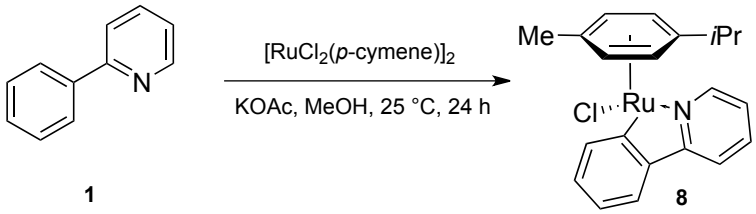

In a Schlenk flask, dinuclear complex [$RuCl_2$(*p*-cymene)]$_2$ (306 mg, 0.5 mmol, 2 equiv. in ruthenium), 2-phenylpyridine **1**(155 mg, 1.0 mmol, 1 equiv.) and KOAc (196.2 mg, 2.0 mmol, 2 equiv.) were solubilized in dry methanol (25 mL) and stirred 24h at room temperature. The solvent was removed under vacuum and the crude was purified by silica gel flash chromatography (PE/AcOEt 3:7) to afford the compound **8** (259 mg, 61%) as a green solid. ^{1}H NMR (300 MHz, $CDCl_3$): δ (ppm) = 9.23 (d, *J*(H,H) = 5.9 Hz, 1H, *H*^{Ar}), 8.15 (d, *J*(H,H) = 7.5 Hz, 1H, *H*^{Ar}), 7.75-7.55 (m, 3H, *H*^{Ar}), 7.18 (td, *J*(H,H) = 7.3 and 1.3 Hz, 1H, *H*^{Ar}), 7.10-6.95 (m, 2H, *H*^{Ar}), 5.57 (m, 2H, *H*^{Ar}), 5.17 (d, *J*(H,H) = 6.0 Hz, 1H, *H*^{Ar}), 4.98 (d, *J*(H,H) = 5.9 Hz, 1H, *H*^{Ar}), 2.43 (sept, *J*(H,H) = 6.9 Hz, 1H, C*H*(CH_3)$_2$), 2.04 (s, 3H, C-C*H*$_3$), 0.98 (d, *J*(H,H) = 6.9 Hz, 3H, CH(C*H*$_3$)$_2$), 0.88 (d, *J*(H,H) = 6.9 Hz, 3H, CH(C*H*$_3$)$_2$). ^{13}C NMR (75 MHz, $CDCl_3$): δ (ppm) = 181.5 (C-Ru), 165.4 (C^{Ar}), 154.7 (C^{Ar}-H), 143.5 (C^{Ar}), 139.7 (C^{Ar}-H), 136.7 (C^{Ar}-H), 129.5 (C^{Ar}-H), 124.0 (C^{Ar}-H), 122.6 (C^{Ar}-H), 121.5 (C^{Ar}-H), 118.9 (C^{Ar}-H), 104.5 (C^{Ar}), 100.6 (C^{Ar}), 90.9 (C^{Ar}-H), 89.7 (C^{Ar}-H), 84.3 (C^{Ar}-H), 82.3 (C^{Ar}-H), 30.9 (CH), 22.6 (CH_3), 21.8 (CH_3), 18.9 (CH_3).

XI. References

1 C. A. Busacca, J. C. Lorenz, N. Grinberg, N. Haddad, M. Hrapchak, B. Latli, H. Lee, P. Sabila, A. Saha, M. Sarvestani, S. Shen, R. varsolona, X. Wei and C. H. Senannayake, *Org. Lett.*, **2005**, *7*, 4277-4280.

2 A. Leyris, J. Bigeault, D. Nuel, L. Giordano and G. Buono, *Tetrahedron Lett.*, **2007**, *48*, 5247-5250.

3 T. L. Emmick and R. L. Letsinger, *J. Am. Chem. Soc.*, **1968**, *90*, 3459-3465.

4 J. Bigeault, L. Giordano, G. Buono, *Angew. Chem. Int. Ed.* **2005**, *44*, 4753-4757.

5 D. D. Perrin and W. L. F. Armarego in *Purification of Laboratory Chemicals*, Pergamnon Press: Oxford, 3rd ed., **1988**.

6 G. R. Fulmer, A. J. M. Miller, N. H. Sherden, H. E. Gottlieb, A. Nudelman, B. M. Stoltz, J. E. Bercaw and K. I. Golberg, *Organometallics*, **2010**, *29*, 2176-2179.

7 A. Altomare, G. Cascarano, C. Giacovazzo and A. Guagliardi, *J. Appl. Cryst.* **1993**, *26*, 343-350.

8 G. M. Shelcrick, *Acta Cryst.* **2008**, *A64*, 112-122.

9 A. Demonceau, A. W. Stumpf, E. Saive and A. F. Noels, *Macromolecules*, **1997**, *30*, 3127-3136.

10 E. Hodson and S. J. Simpson, *Polyhedron*, **2004**, *23*, 2695-2707.

11 S. M. M. Knapp, T. J. Sherbow, R. B. Yelle, J. J. Juliette and D. R. Tyler, *Organometallics*, **2013**, *32*, 3744-3752.

12 M. Klinga, A. Abele, R. Wursche and B. Rieger, *Private Communication*, **1999**.

13 S. E. Dann, S. E. Durran, M. R. J. Elsegood, M. B. Smith, P. M. Staniland, S. Talib and S. H. Dale, *J. Organomet. Chem.*, **2006**, *691*, 4829-4842.

14 G. Bruno, M. Panzalorto, F. Nicolo, C. G. Arena and P. Cardiano, *Acta Crystallogr., Sect. C: Cryst. Struct. Commun.*, **2000**, *56*, e429.

15 M. R. J. Elsegood, M. B. Smith and N. M. Sanchez-Ballester, *Acta Crystallogr. Sect. E: Struct. Rep. Online*, **2006**, *62*, m2838-m2840.

16 E. Hodson and S. J. Simpson, *Polyhedron*, **2004**, *23*, 2695-2707.

17 A. Hafner, A. Muhlebach and P. A. van der Schaaf, *Angew. Chem. Int. Ed.*, **1997**, *36*, 2121-2124.

18 S. Serron, S. P. Nolan, Y. A. Abramov, L. Brammer and J. L. Petersen, *Organometallics*, **1998**, *17*, 104-110.

19 J. Wolf, K. Thommes, O. Briel, R. Scopelliti and K. Severin, *Organometallics*, **2008**, *27*, 4464-4474.

20 A. Grabulosa, A. Mannu, A. Mezzetti and G. Muller, *J. Organomet. Chem.*, **2012**, *696*, 4221-4228.

21 C. Lo, R. Cariou, C. Fischmeister and P. H. Dixneuf, *Adv. Synth. Catal.*, **2007**, *349*, 546-550.

22 W. A. Herrmann, C. Köcher, L. J. Gooßen and G. R. J. Artus, *Chem. Eur. J.*, **1996**, *2*, 1627-1636.

23 Y. Zhang, C. Chen, S. C. Ghosh, Y. Li and S. H. Hong, *Organometallics*, **2010**, *29*, 1374-1378

24 N. Gürbüz, E. Ö. Özcan, I. Özdemir, B. Çetinkaya, O. Sahin and O. Büyükgüngör, *Dalton Trans.*, **2012**, *41,* 2330-2339.

25 F. Schröder, C. Tugny, E. Salanouve, H. Clavier, L. Giordano, D. Moraleda, Y. Gimbert, V. Mouriès-Mansuy, J-P. Goddard and L. Fensterbank, *Organometallics*, **2014**, *33*, 4051-4056.

26 I. J. S. Fairlamb, S. Grant, A. C. Whitwood, J. Whitthall, A. S. Batsanov and J. C. Collings, *J. Organomet. Chem.*, **2005**, *690*, 4462-4477.

27 T. Achard, L. Giordano, A. Tenaglia, Y. Gimbert and G. Buono, *Organometallics*, **2010**, *29*, 3936-3950.

28 G. Y. Li, *J. Org. Chem.*, **2002**, *67*, 3643-3650.

29 J. Kanada and M. Tanaka, *Adv. Synth. Catal.*, **2011**, *353*, 890-896.

30 L. Ackermann, H. K. Potukuchi, A. R. Kapdi and C. Schulzke, *Chem. Eur. J.*, **2010**, *16*, 3300-3303.

31 L. Ackermann, *Org. Lett.*, **2005**, *7*, 3123-3125.

32 A. Neels, H. Stoeckli-Evans, L. Plasseraud, E. G. Fidalgo and G. Süss-Fink, *Acta Cryst.* **1999**, *C55*, 2030-2032.

33 B. Li, T. Roisnel, C. Darcel and P. H. Dixneuf, *Dalton Trans.*, **2012**, *41*, 10934-10937.

XII. NMR spectra of new products

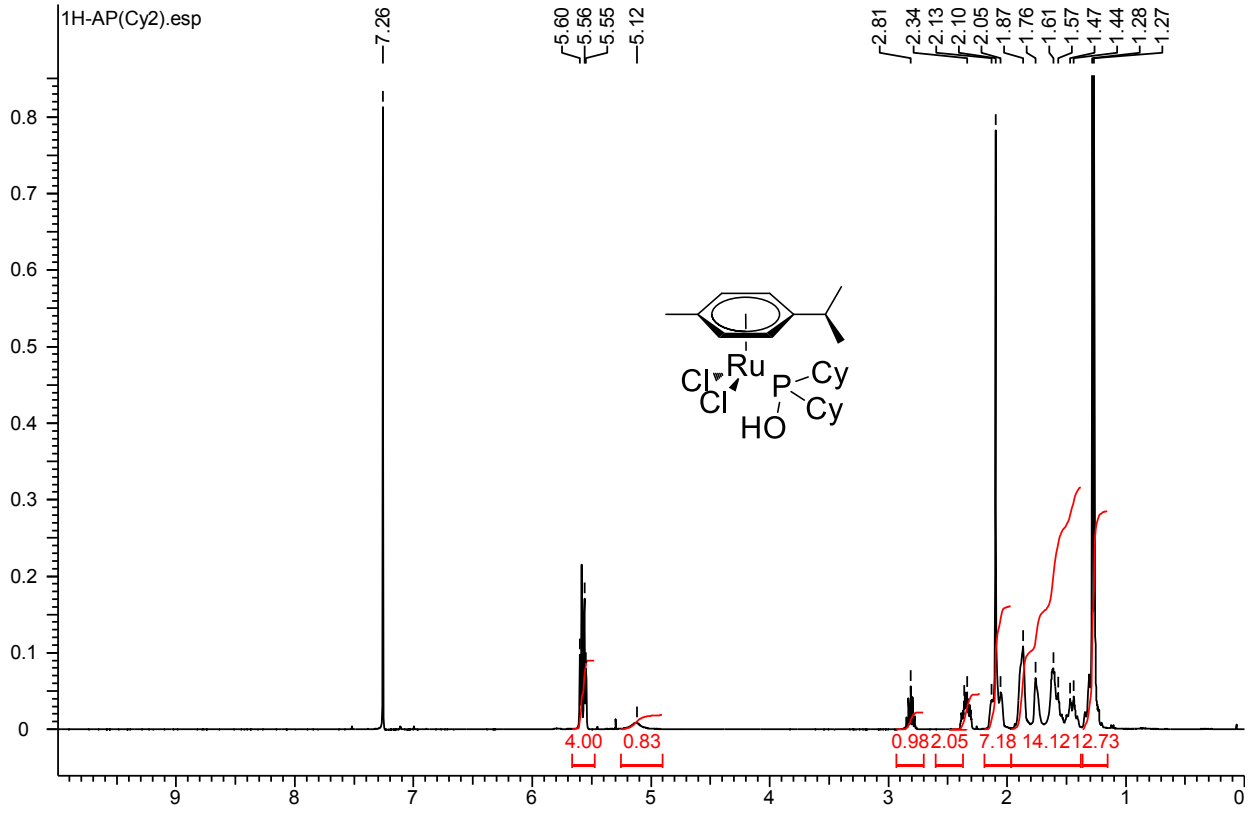

Figure 1. ^{1}H NMR spectrum (400 MHz, $CDCl_3$) of [$RuCl_2$(*p*-cymene)(Cy_2POH)] **5b**

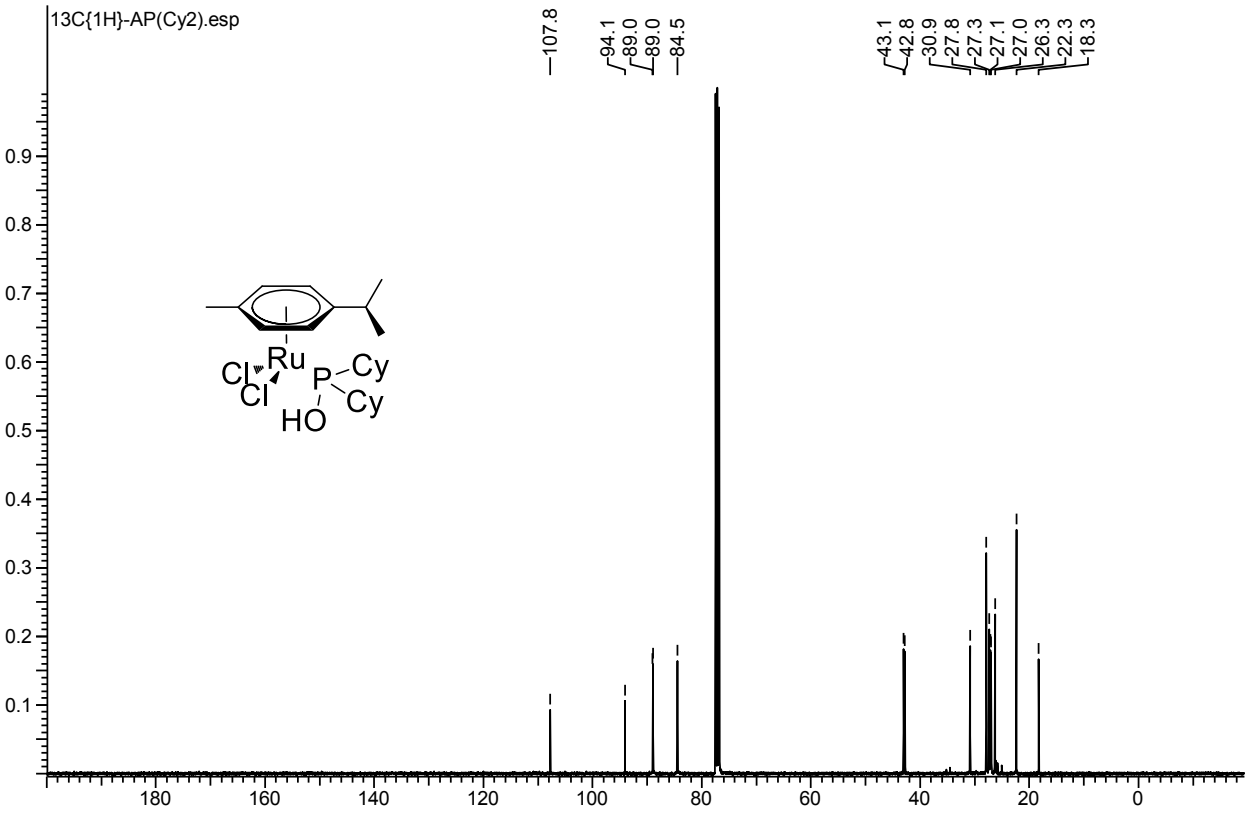

Figure 2. $^{13}C\{^{1}H\}$ NMR spectrum (101 MHz, $CDCl_3$) of [$RuCl_2$(*p*-cymene)(Cy_2POH)] **5b**

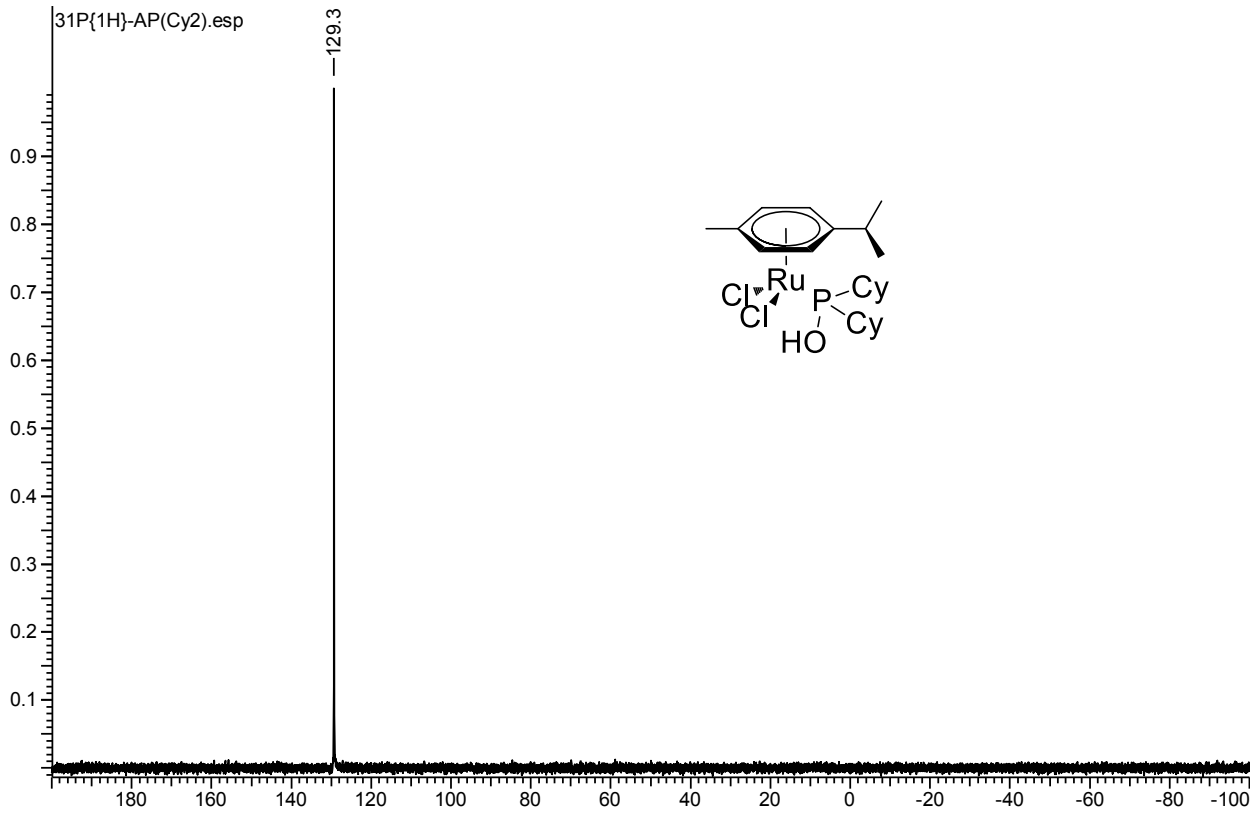

Figure 3. $^{31}P\{^{1}H\}$ NMR spectrum (162 MHz, $CDCl_3$) of [$RuCl_2$(*p*-cymene)(Cy_2POH)] **5b**

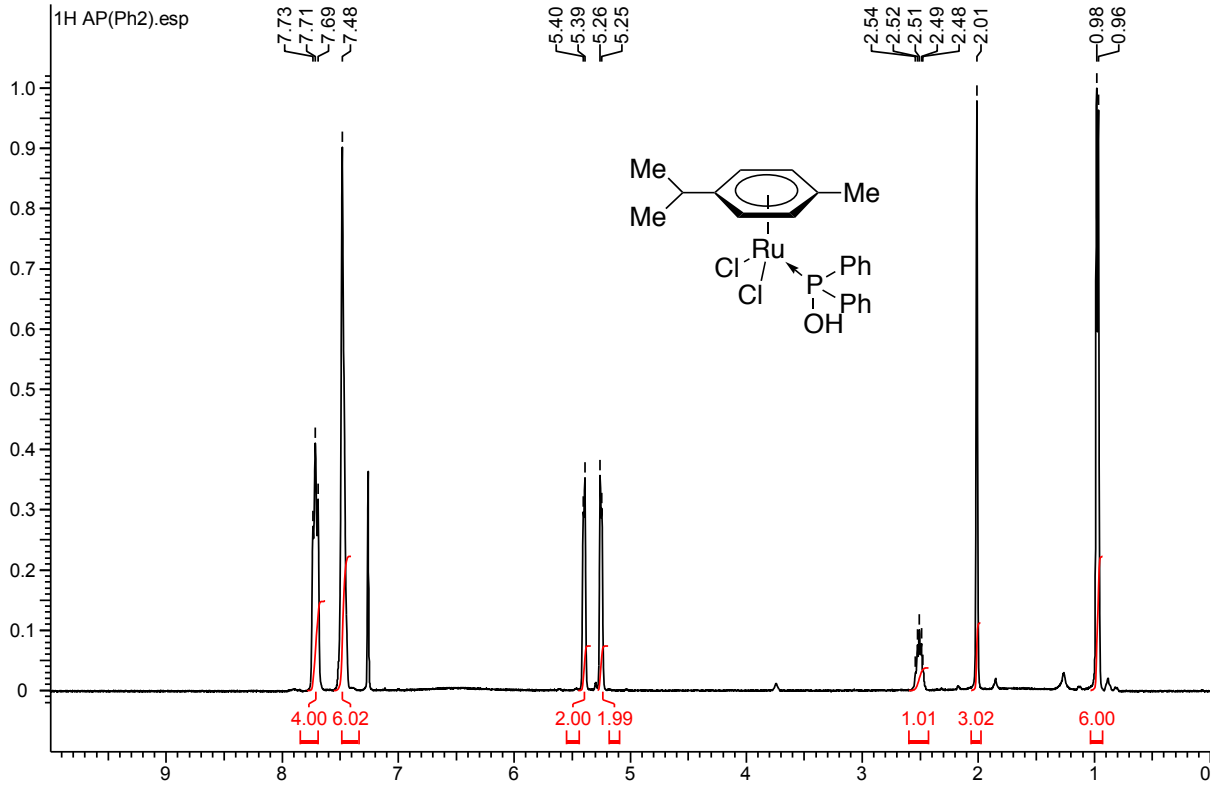

Figure 4. ^{1}H NMR spectrum (400 MHz, $CDCl_3$) of [$RuCl_2$(*p*-cymene)(Ph_2POH)] **5c**

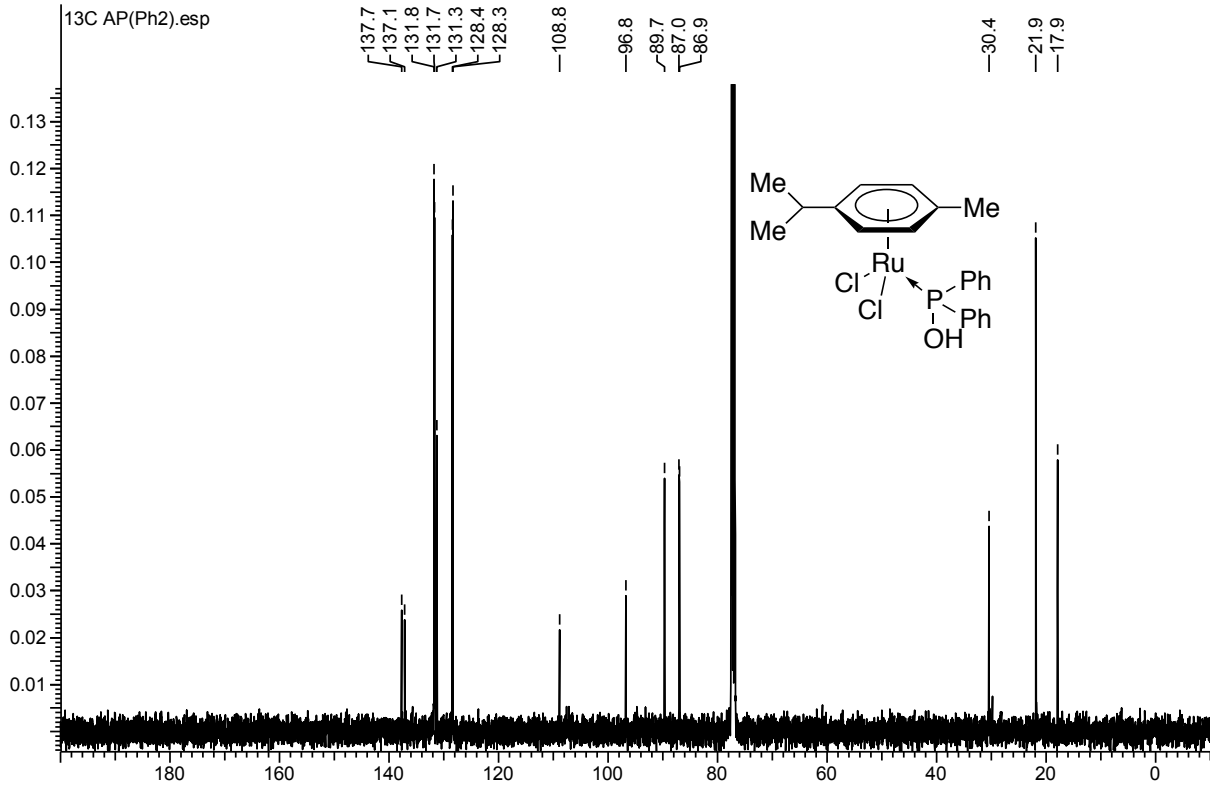

Figure 5. $^{13}C\{^{1}H\}$ NMR spectrum (101 MHz, $CDCl_3$) of $[RuCl_2(p\text{-cymene})(Ph_2POH)]$ **5c**

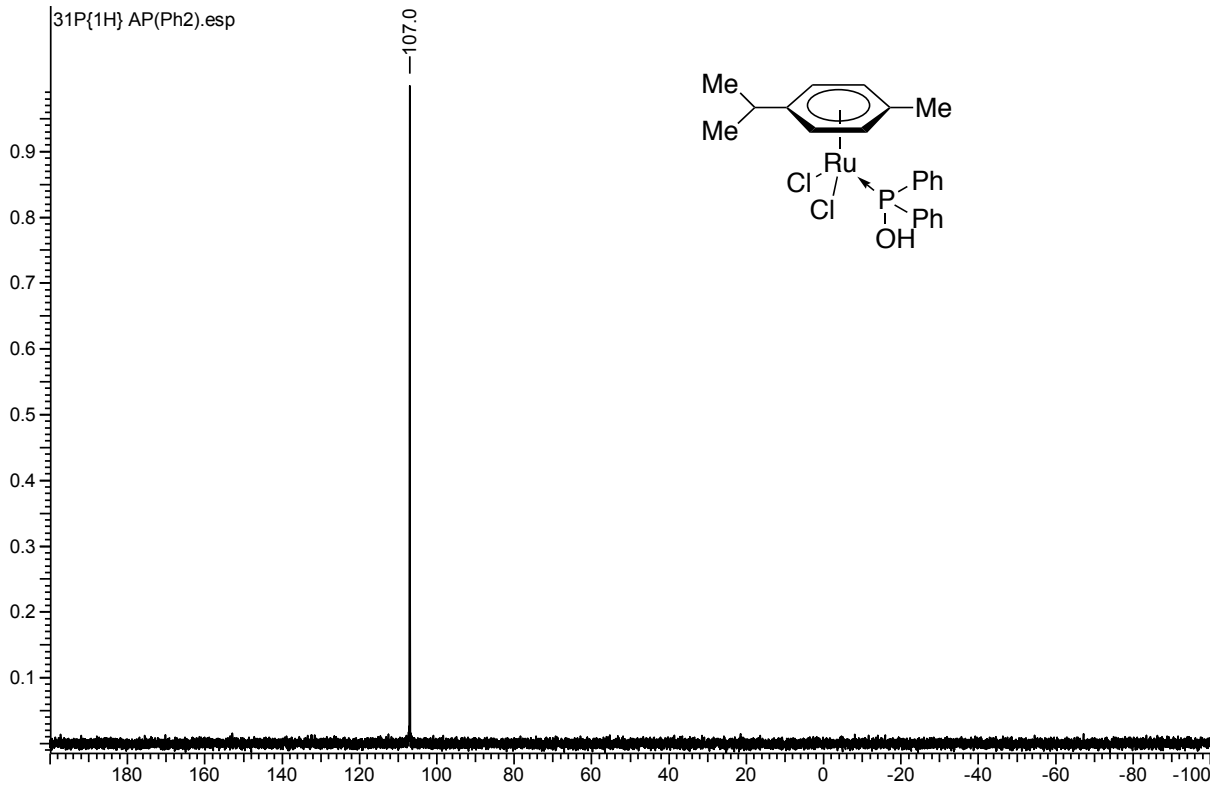

Figure 6. $^{31}P\{^{1}H\}$ NMR spectrum (162 MHz, $CDCl_3$) of $[RuCl_2(p\text{-cymene})(Ph_2POH)]$ **5c**

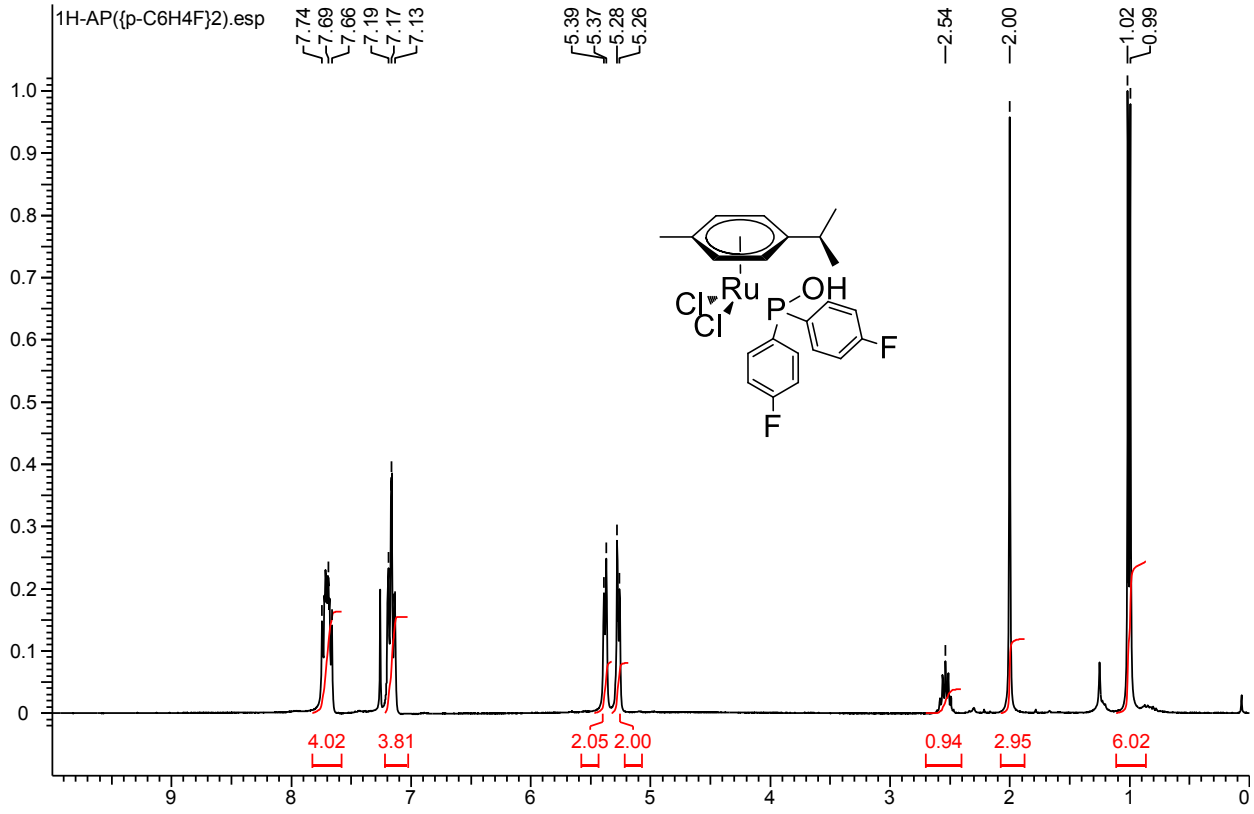

Figure 7. ^{1}H NMR spectrum (400 MHz, $CDCl_3$) of [$RuCl_2$(η^6-*p*-cymene)({4-fluorophenyl}$_2$POH)] **5d**

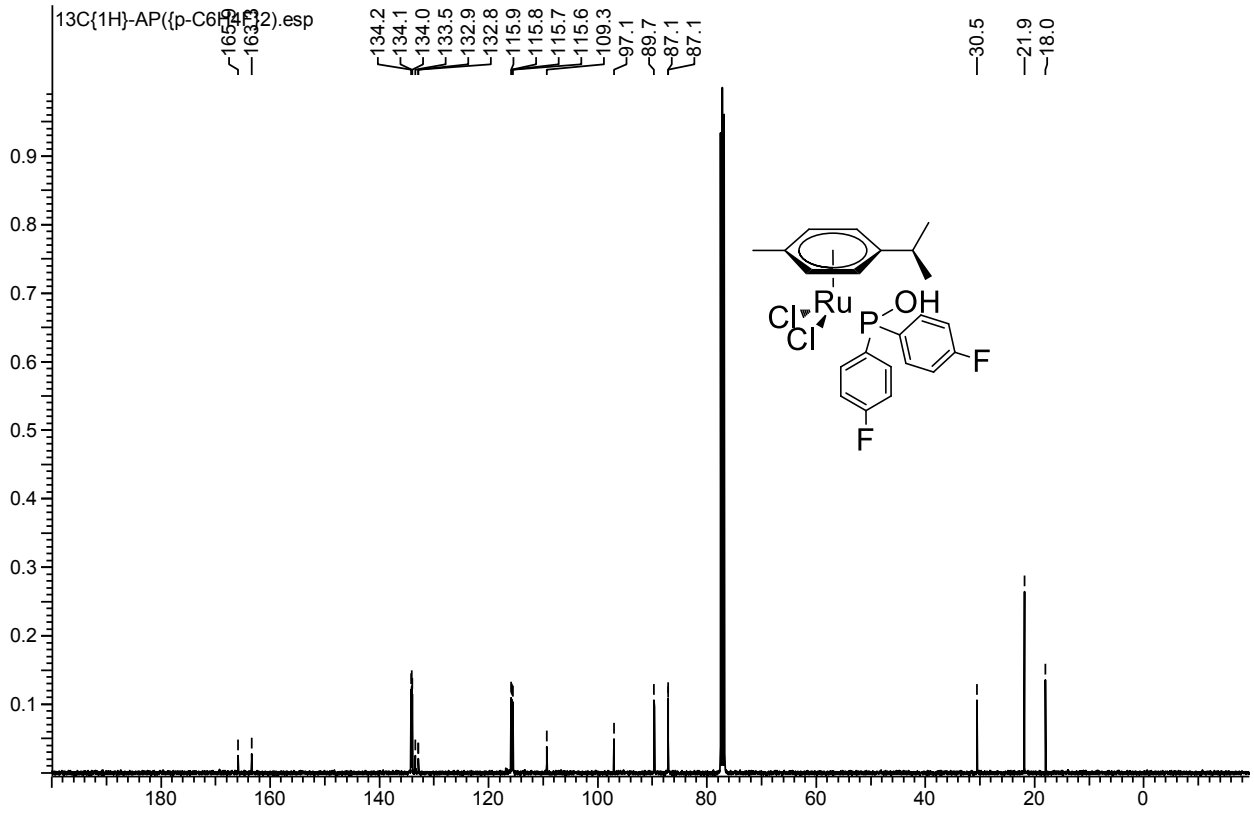

Figure 8. ^{13}C{^{1}H} NMR spectrum (101 MHz, $CDCl_3$) of [$RuCl_2$(η^6-*p*-cymene)({4-fluorophenyl}$_2$POH)] **5d**

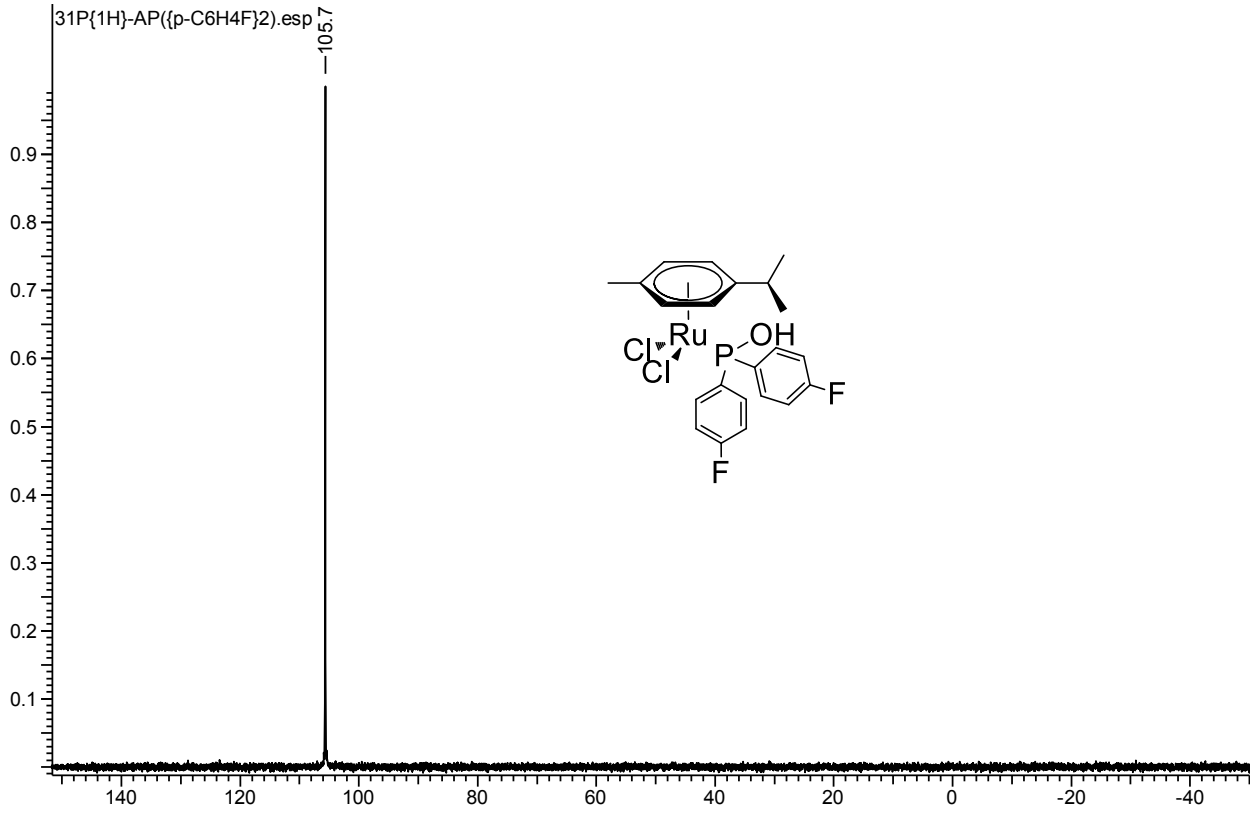

Figure 9. $^{31}P\{^{1}H\}$ NMR spectrum (162 MHz, $CDCl_3$) of [$RuCl_2$(η^6-*p*-cymene)({4-fluorophenyl}$_2$POH)] **5d**

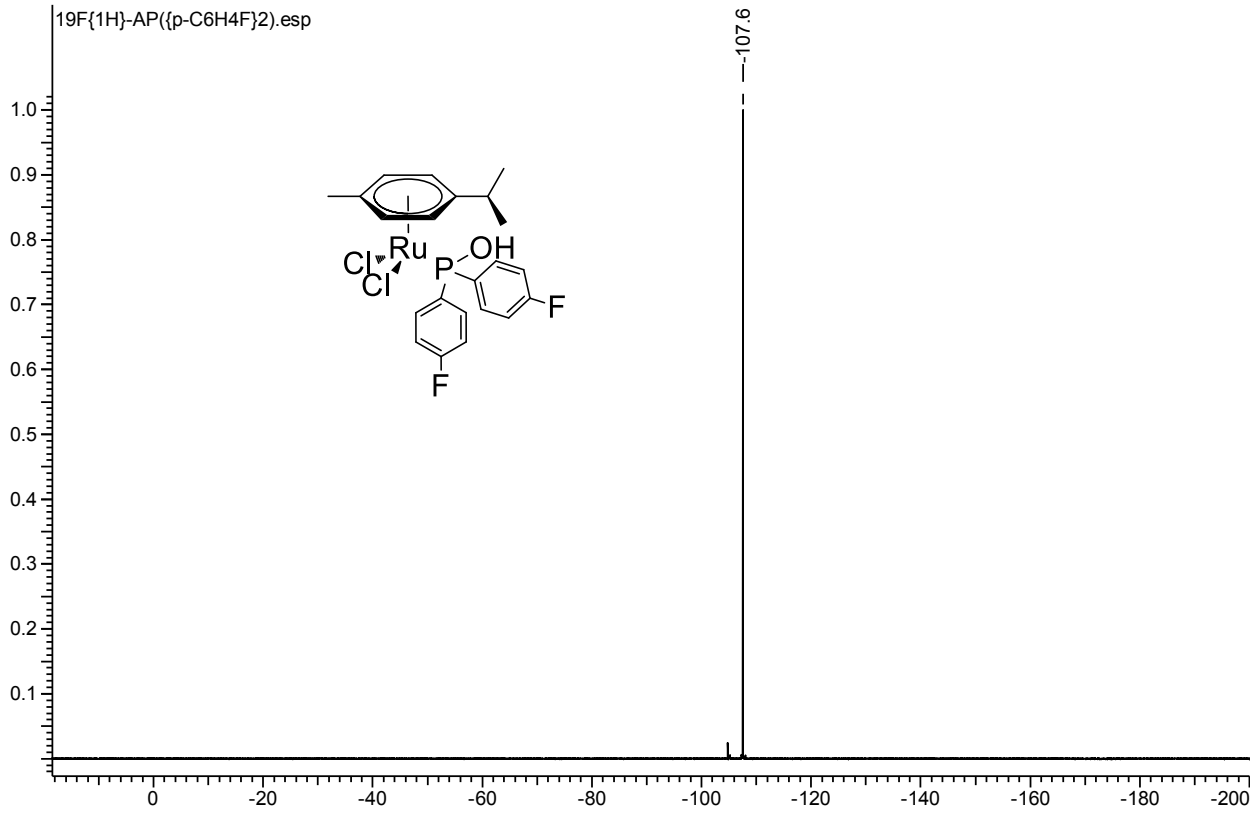

Figure 10. $^{19}F\{^{1}H\}$ NMR spectrum (377 MHz, $CDCl_3$) of [$RuCl_2$(η^6-*p*-cymene)({4-fluorophenyl}$_2$POH)] **5d**

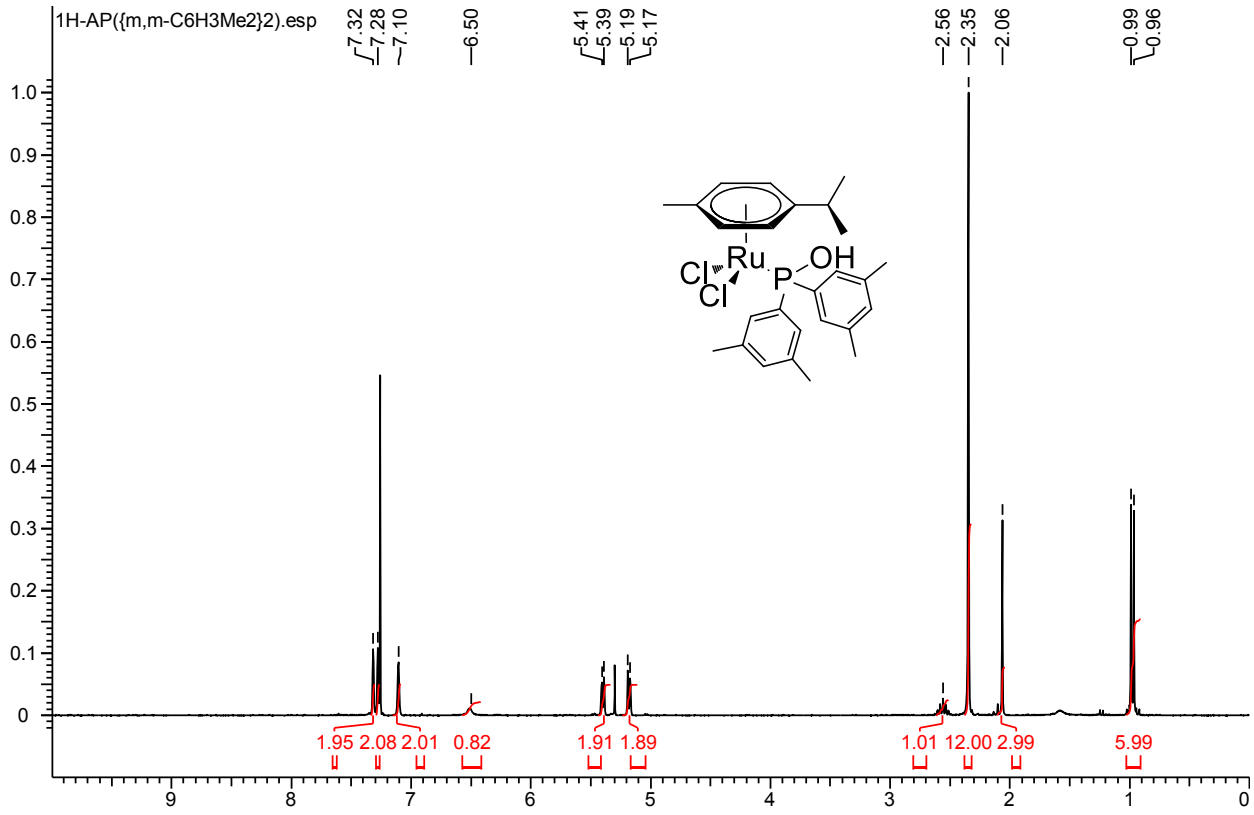

Figure 11. ^{1}H NMR spectrum (300 MHz, $CDCl_3$) of [$RuCl_2$(η^6-*p*-cymene)({3,5-dimethylphenyl}$_2$POH)] **5e**

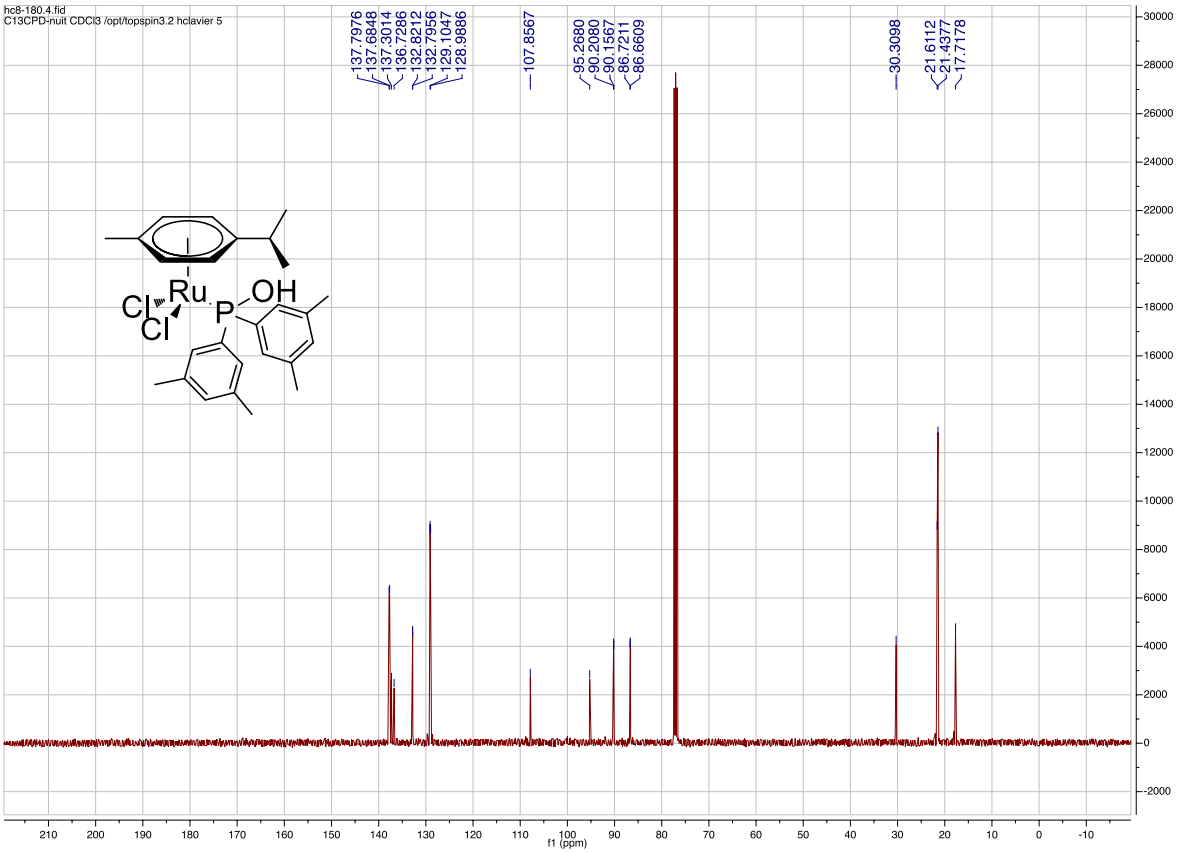

Figure 12. ^{13}C NMR spectrum (100 MHz, $CDCl_3$) of [$RuCl_2$(η^6-*p*-cymene)({3,5-dimethylphenyl}$_2$POH)] **5e**

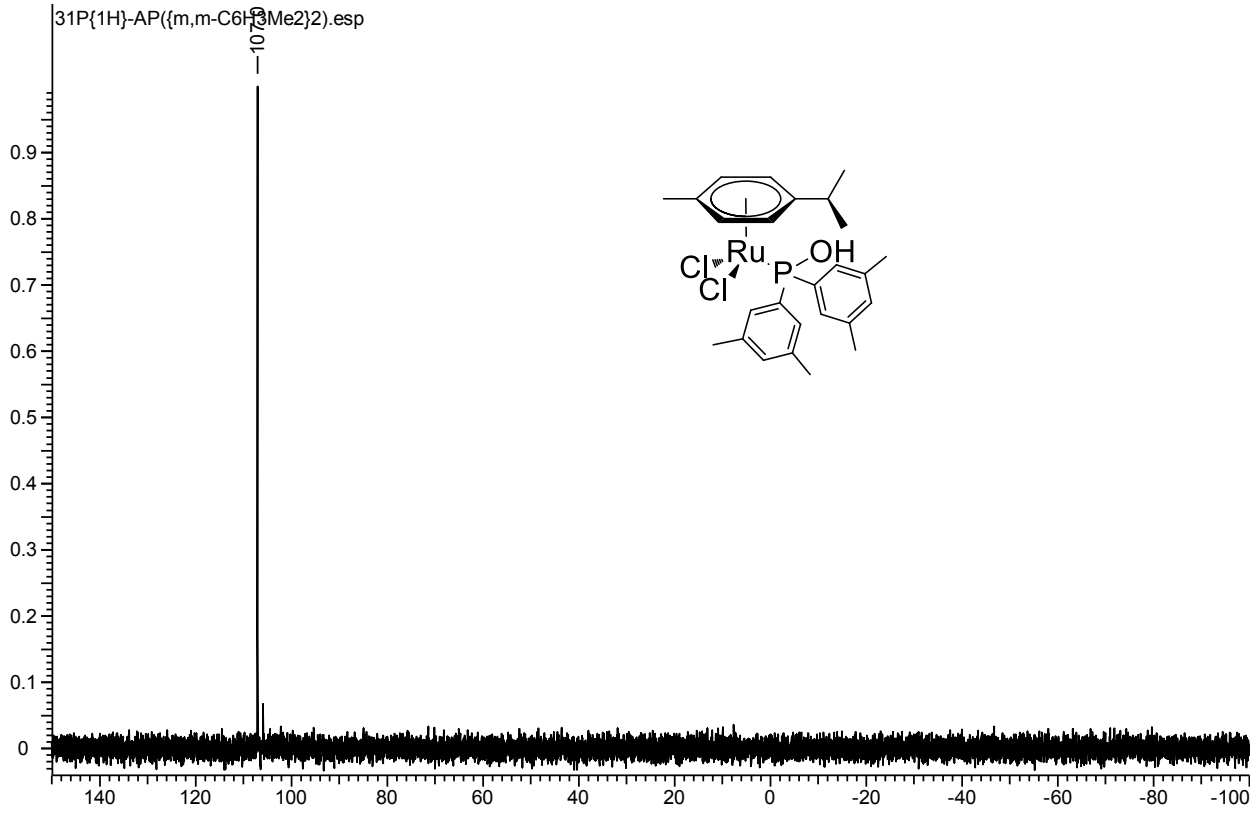

Figure 13. $^{31}P\{^{1}H\}$ NMR spectrum (121 MHz, $CDCl_3$) of [$RuCl_2$(η^6-*p*-cymene)({3,5-dimethylphenyl}$_2$POH)] **5e**

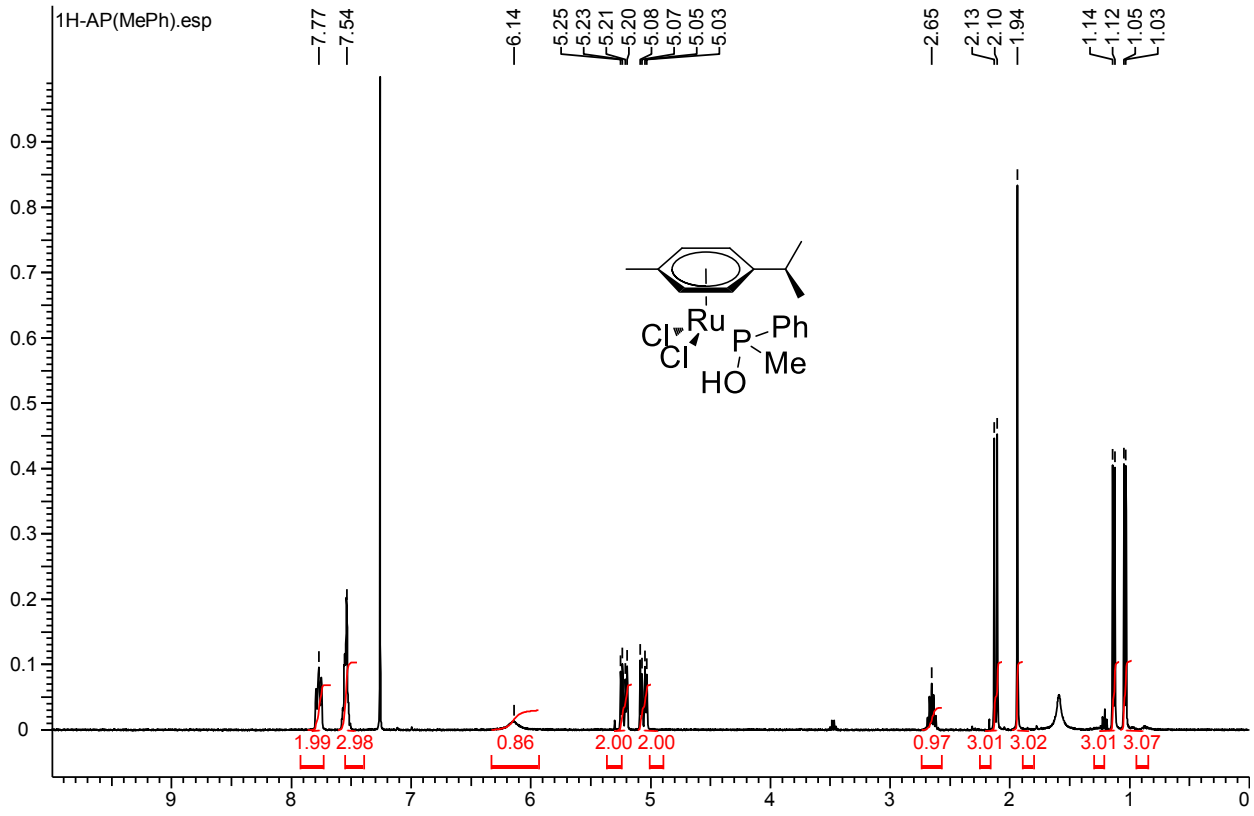

Figure 14. ^{1}H NMR spectrum (400 MHz, $CDCl_3$) of [$RuCl_2$(*p*-cymene)(MePhPOH)] **5h**

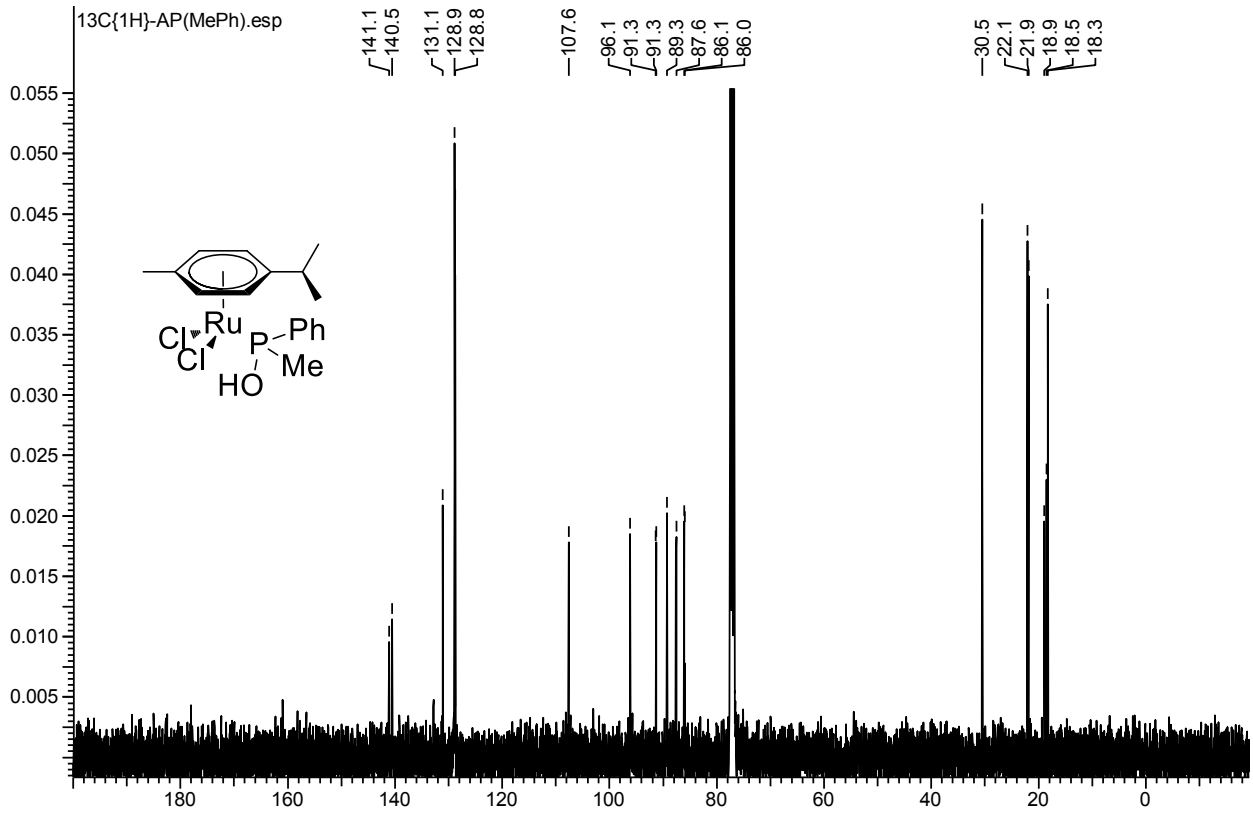

Figure 15. $^{13}C\{^{1}H\}$ NMR spectrum (101 MHz, $CDCl_3$) of [$RuCl_2$(*p*-cymene)(MePhPOH)] **5h**

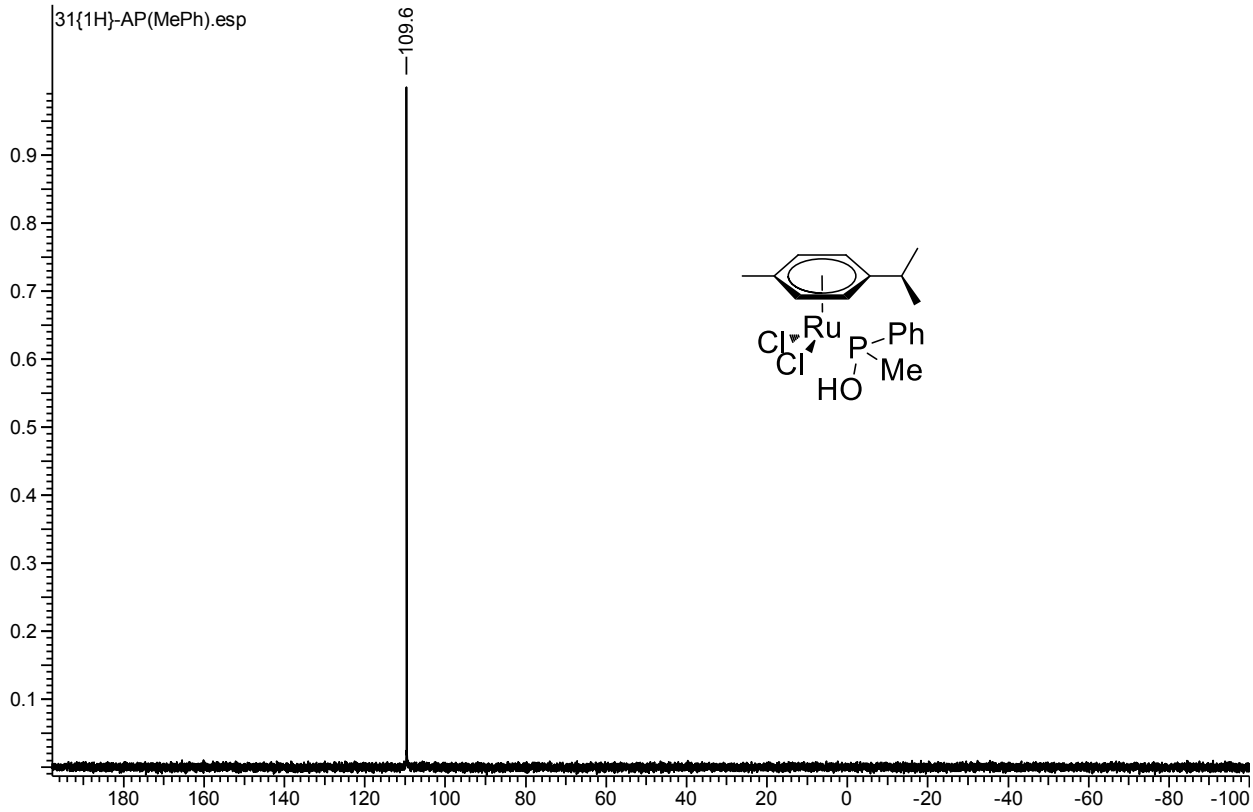

Figure 16. $^{31}P\{^{1}H\}$ NMR spectrum (162 MHz, $CDCl_3$) of [$RuCl_2$(*p*-cymene)(MePhPOH)] **5h**

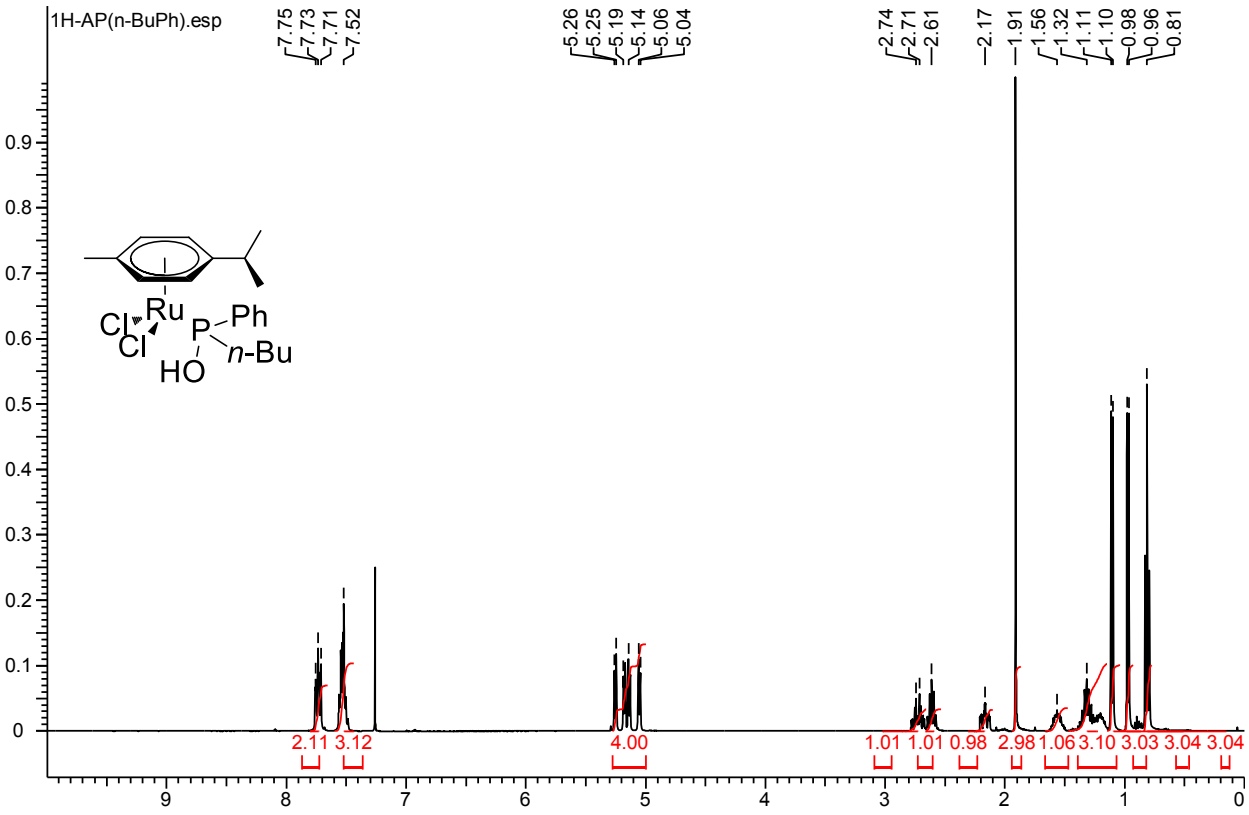

Figure 17. ^{1}H NMR spectrum (400 MHz, $CDCl_3$) of [$RuCl_2$(*p*-cymene)(*n*-BuPhPOH)] **5i**

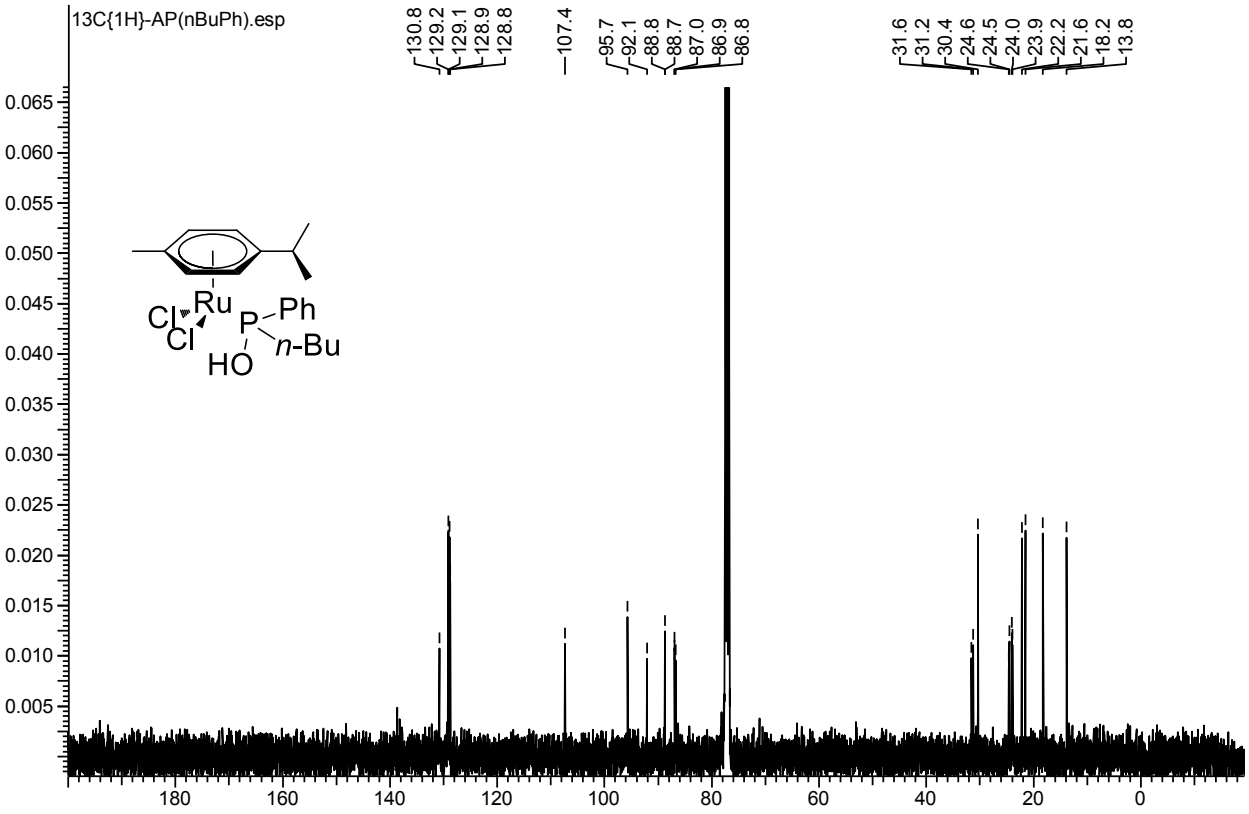

Figure 18. $^{13}C\{^{1}H\}$ NMR spectrum (101 MHz, $CDCl_3$) of [$RuCl_2$(*p*-cymene)(*n*-BuPhPOH)] **5i**

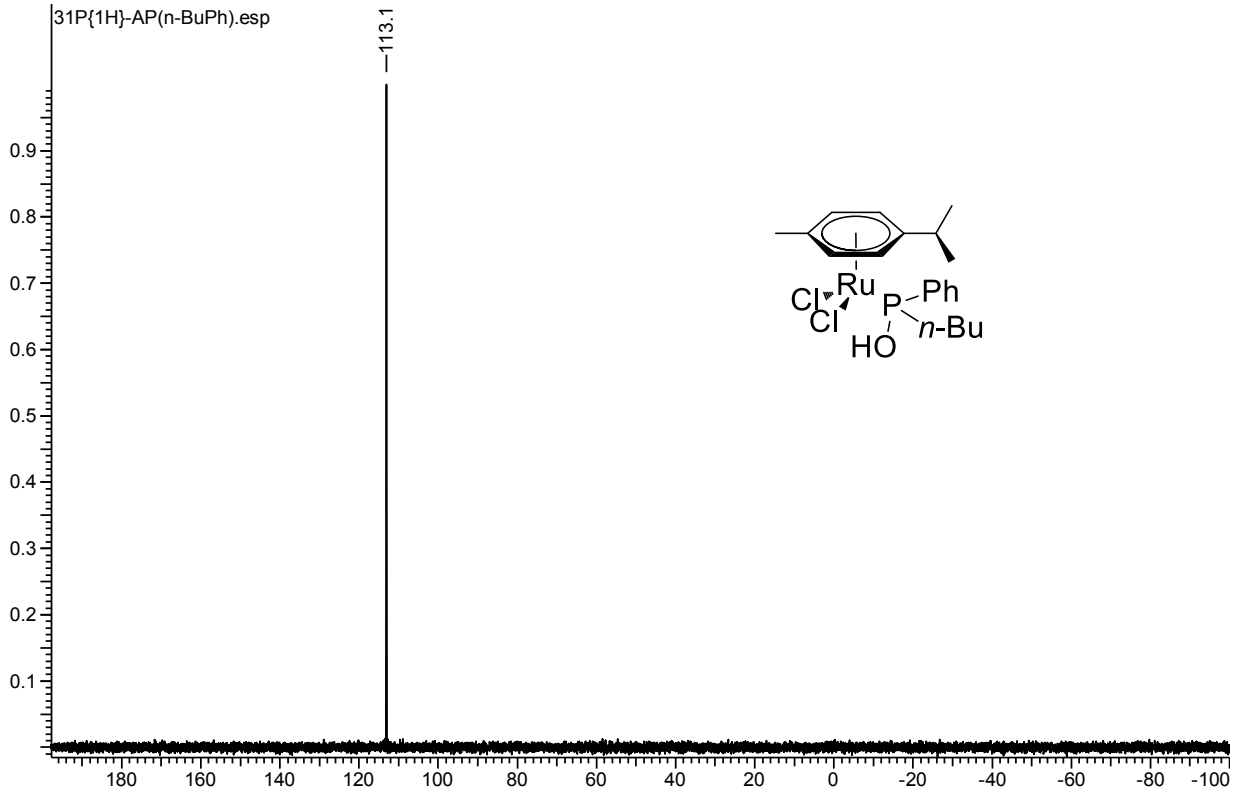

Figure 19. $^{31}P\{^{1}H\}$ NMR spectrum (162 MHz, $CDCl_3$) of [$RuCl_2$(*p*-cymene)(*n*-BuPhPOH)] **5i**

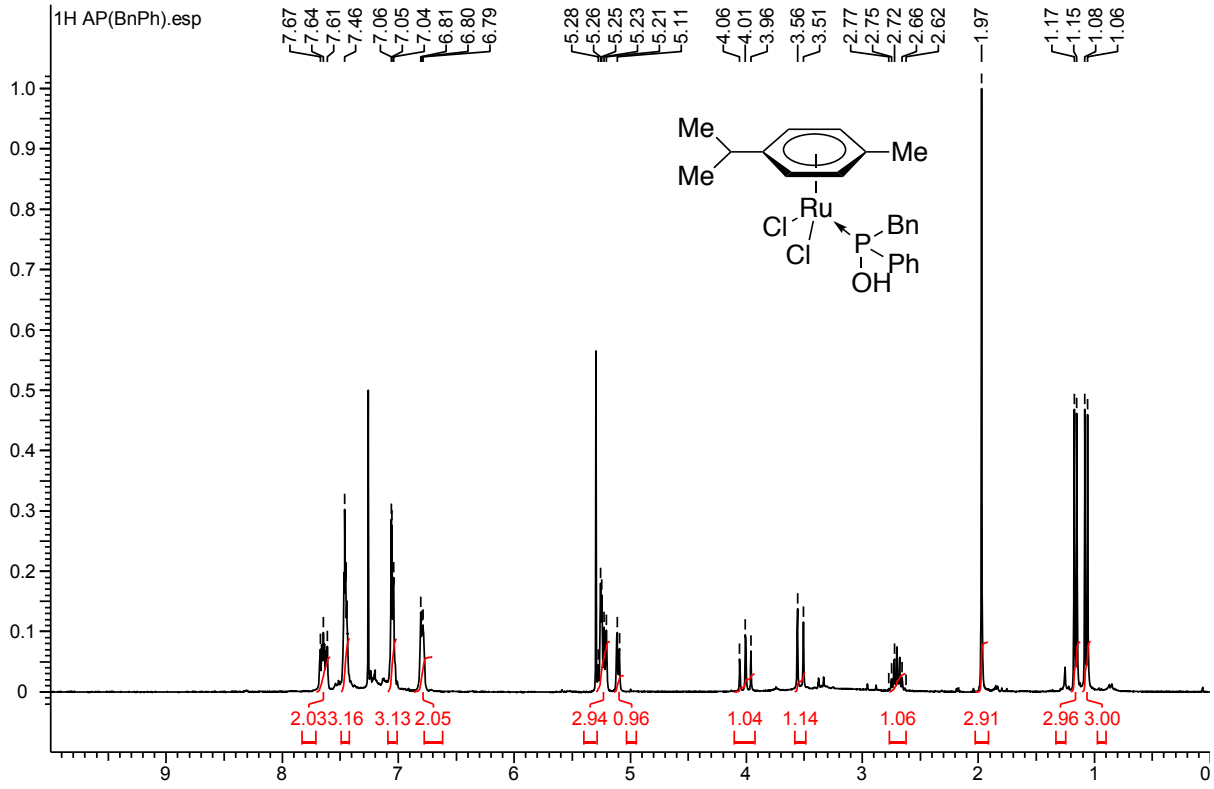

Figure 20. ^{1}H NMR spectrum (300 MHz, $CDCl_3$) of [$RuCl_2$(*p*-cymene)(BnPhPOH)] **5j**

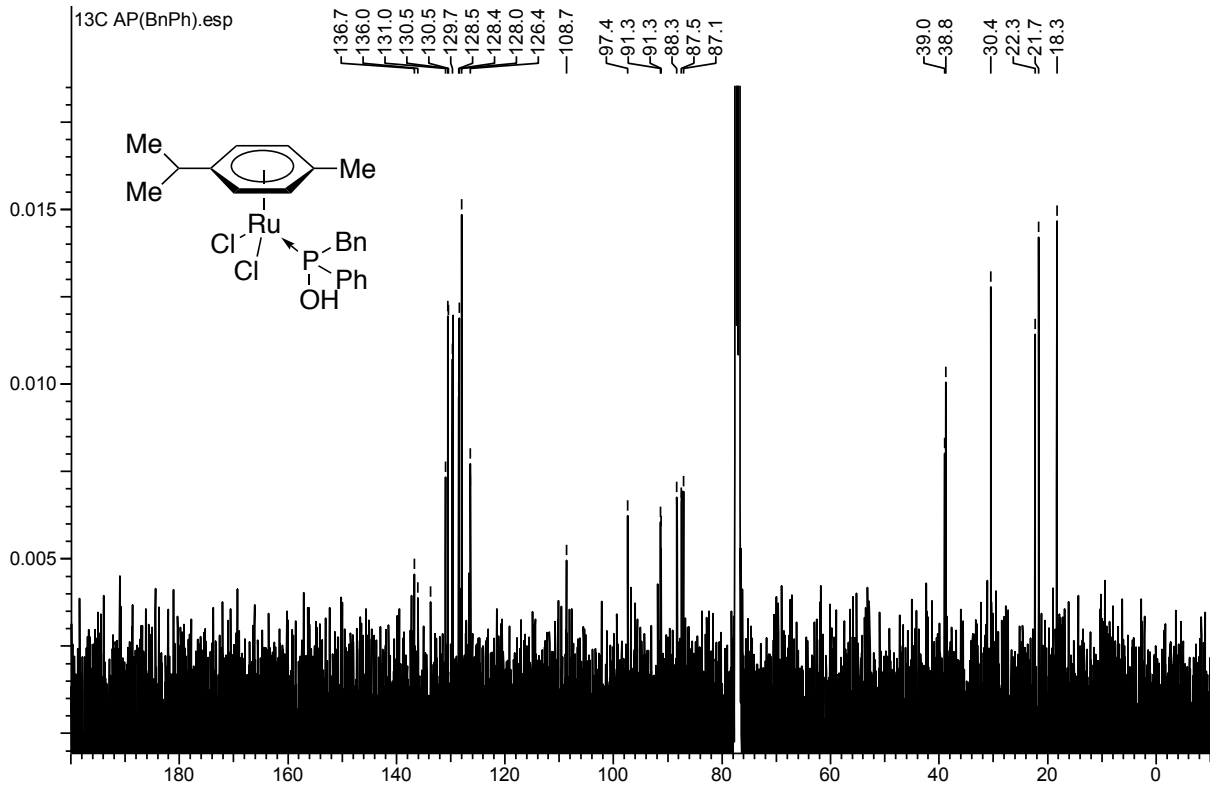

Figure 21. $^{13}C\{^{1}H\}$ NMR spectrum (101 MHz, $CDCl_3$) of [$RuCl_2$(*p*-cymene)(BnPhPOH)] **5j**

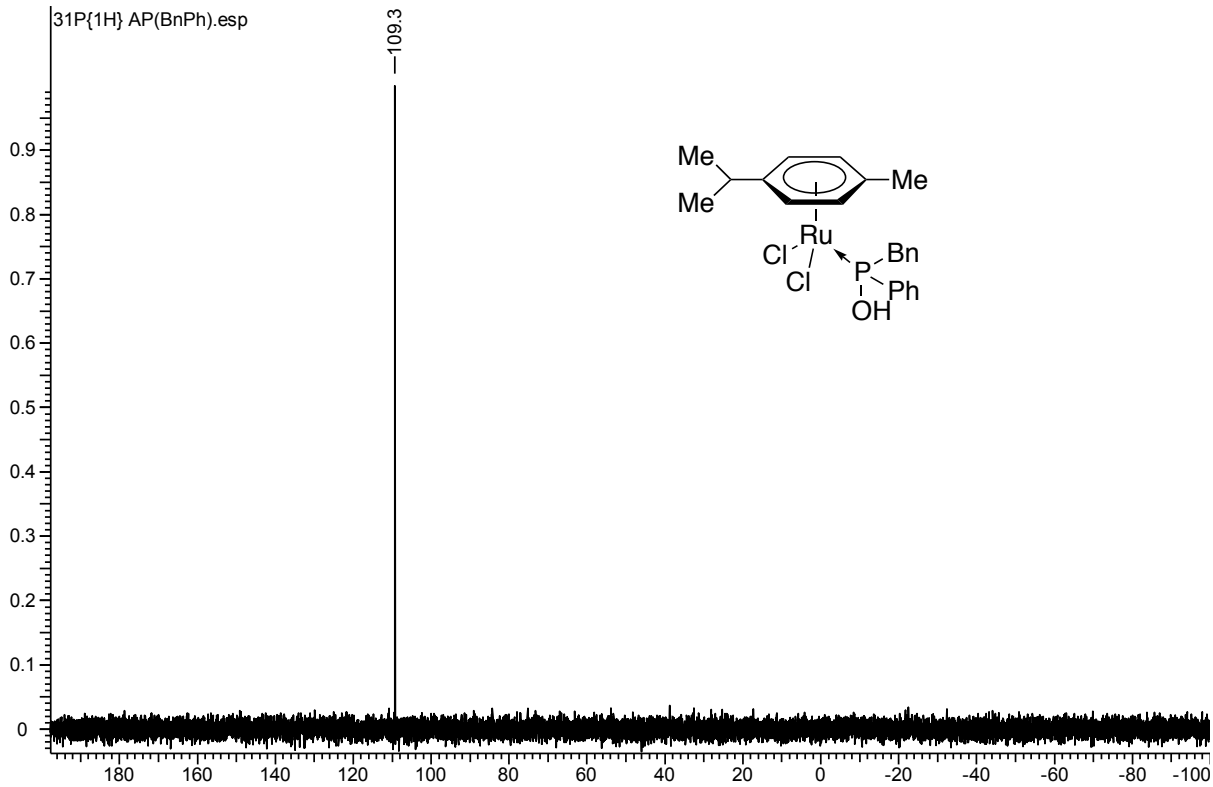

Figure 22. $^{31}P\{^{1}H\}$ NMR spectrum (121 MHz, $CDCl_3$) of [$RuCl_2$(*p*-cymene)(BnPhPOH)] **5j**

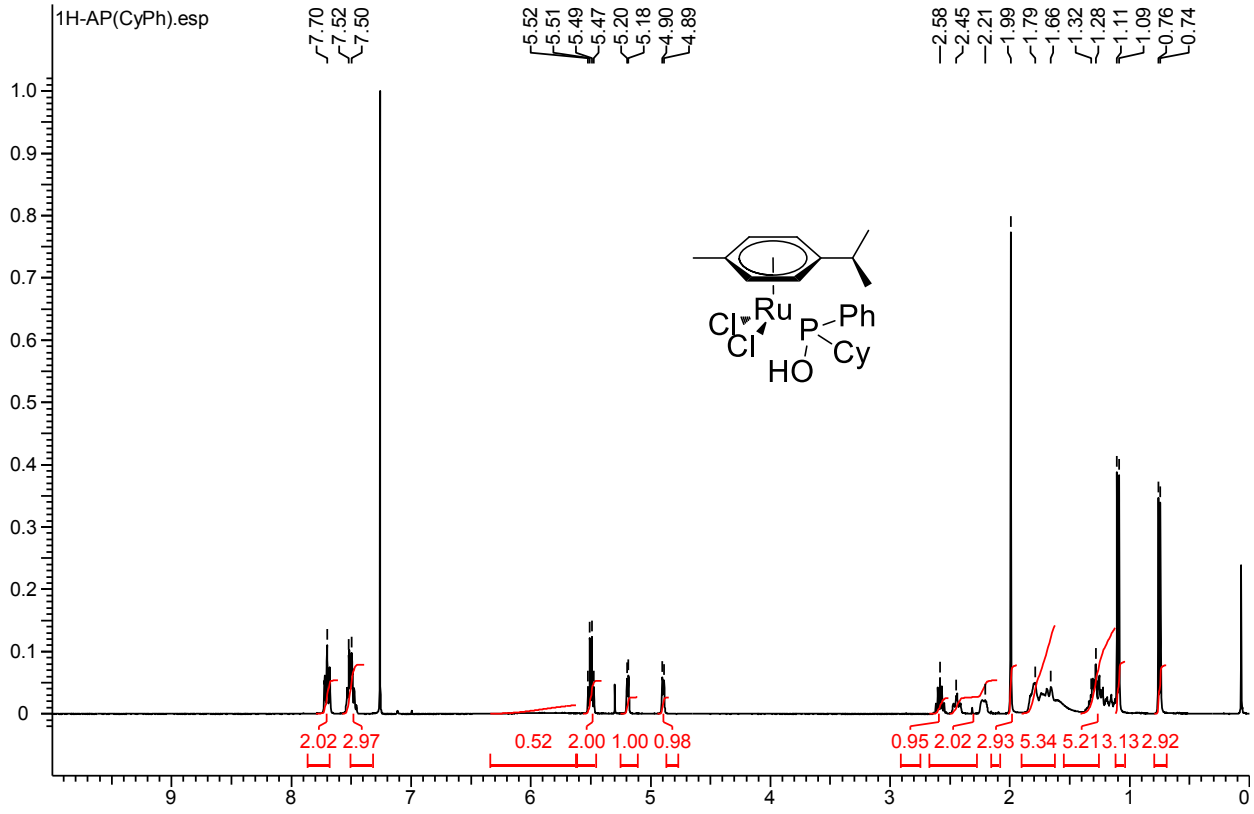

Figure 23. ^{1}H NMR spectrum (400 MHz, $CDCl_3$) of [$RuCl_2$(*p*-cymene)(CyPhPOH)] **5k**

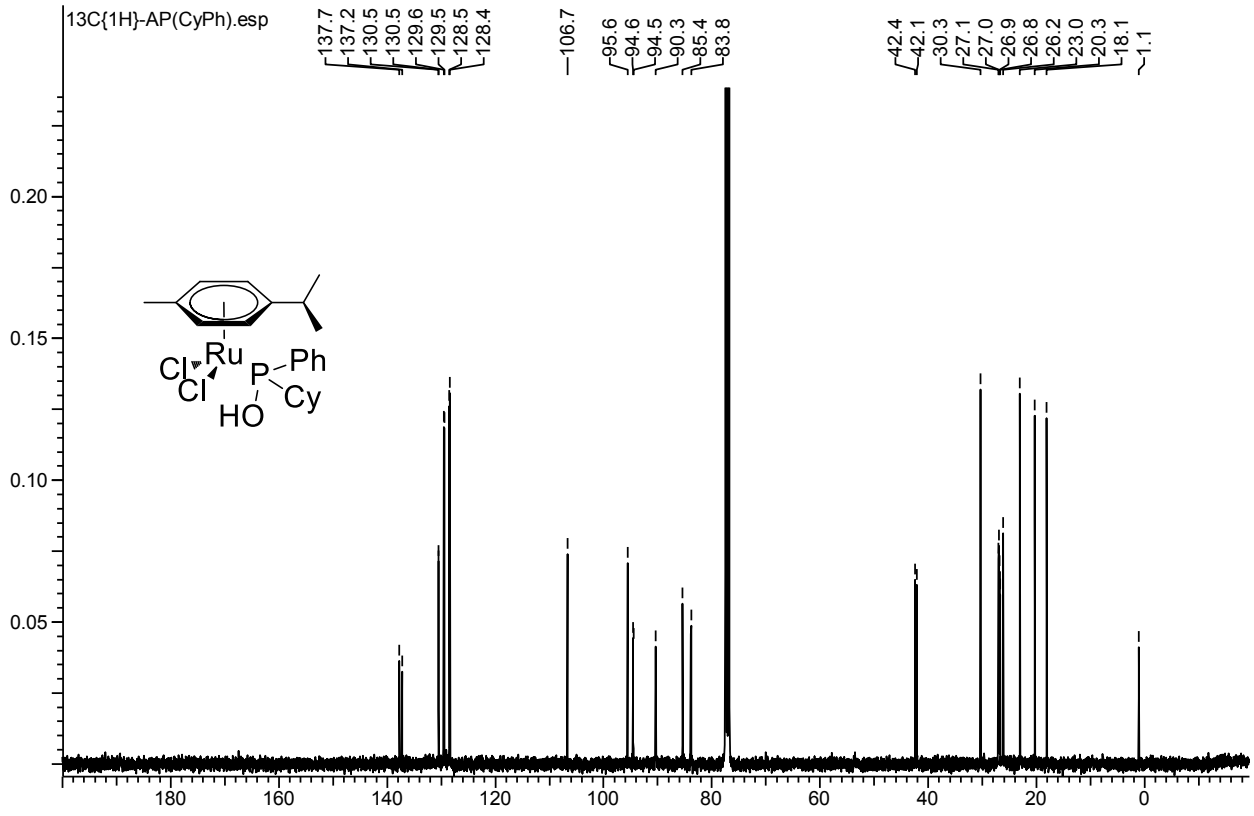

Figure 24. $^{13}C\{^{1}H\}$ NMR spectrum (121 MHz, $CDCl_3$) of [$RuCl_2$(*p*-cymene)(CyPhPOH)] **5k**

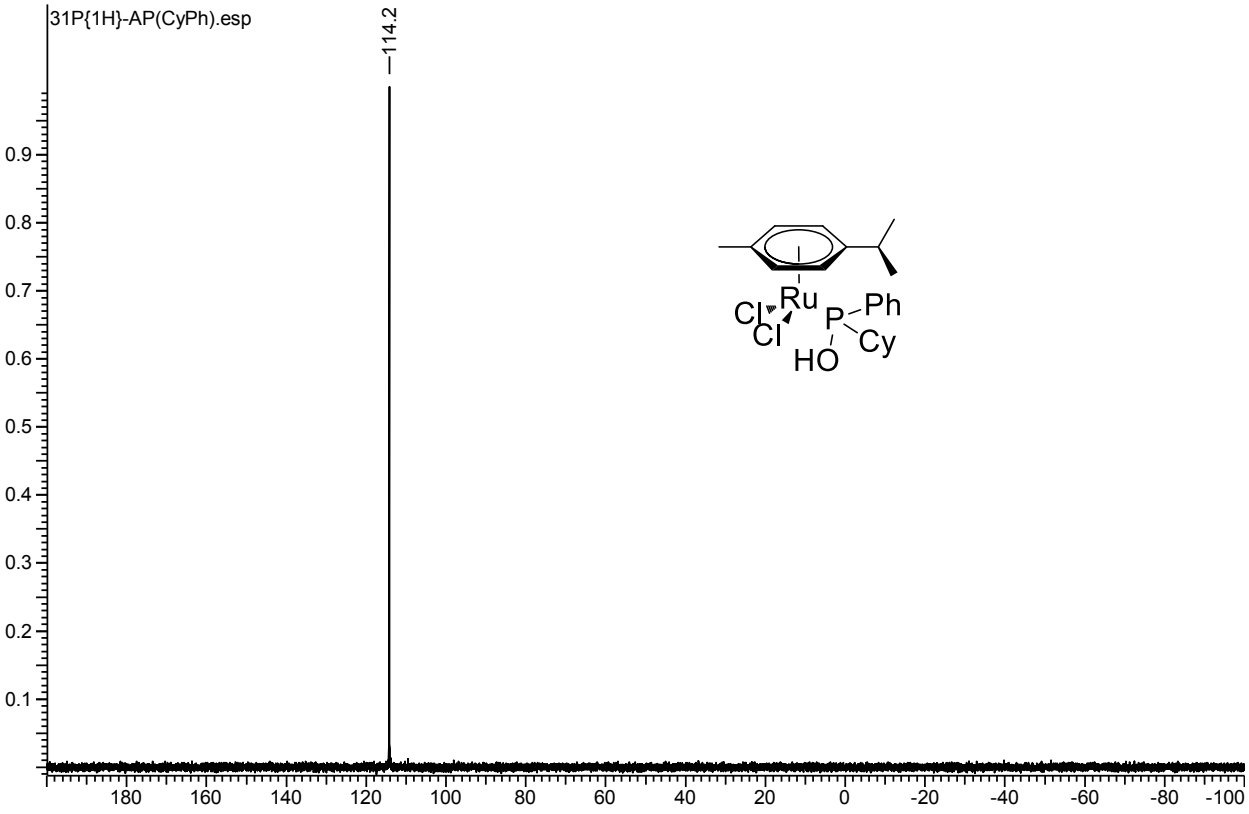

Figure 25. $^{31}P\{^{1}H\}$ NMR spectrum (162 MHz, $CDCl_3$) of [$RuCl_2$(*p*-cymene)(CyPhPOH)] **5k**

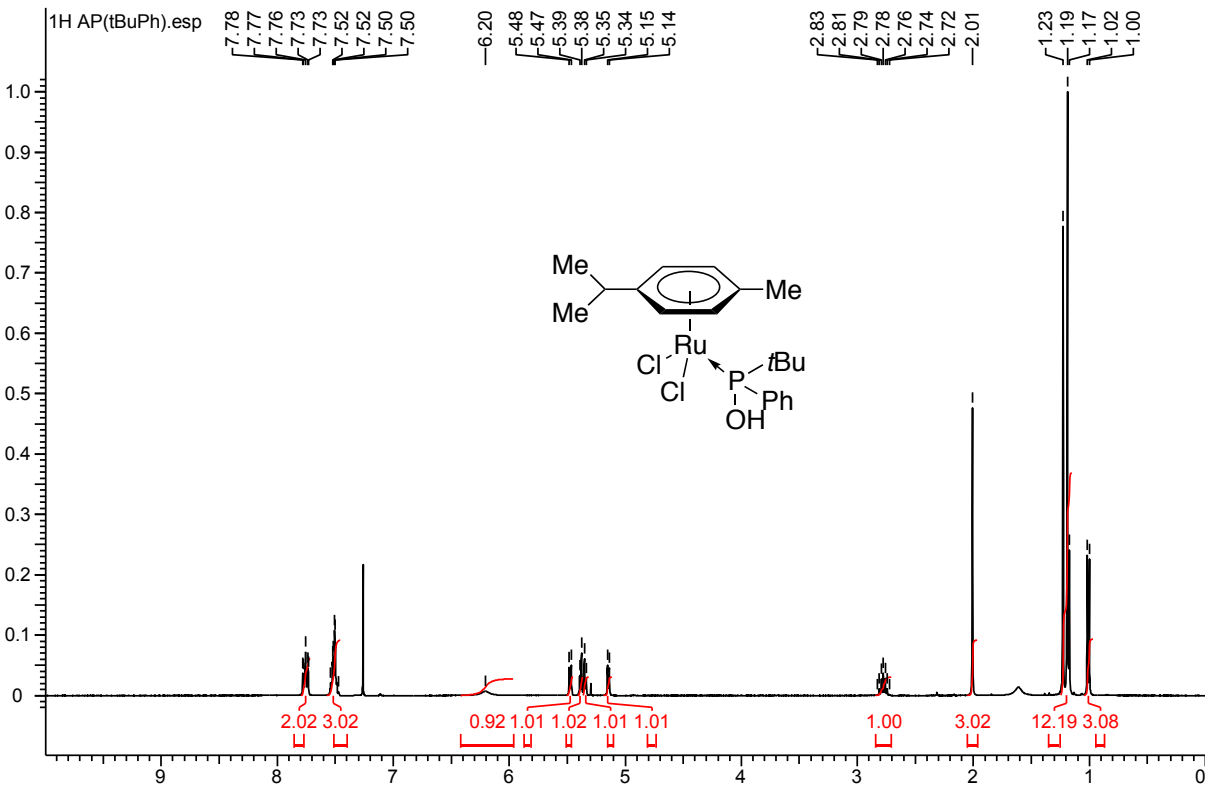

Figure 26. ^{1}H NMR spectrum (400 MHz, $CDCl_3$) of [$RuCl_2$(η^6-*p*-cymene)(*t*-BuPhPOH)] **5l**

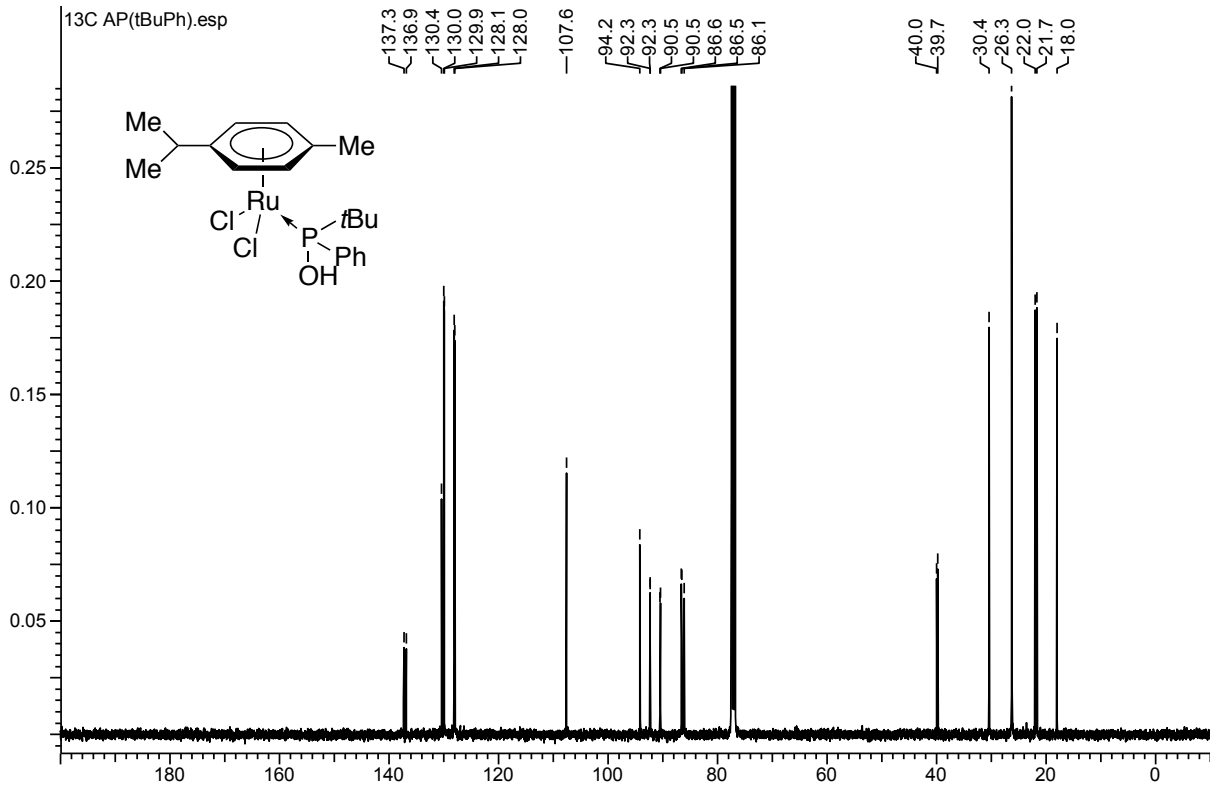

Figure 27. $^{13}C\{^{1}H\}$ NMR spectrum (100 MHz, $CDCl_3$) of [$RuCl_2$(η^6-*p*-cymene)(*t*-BuPhPOH)] **5l**

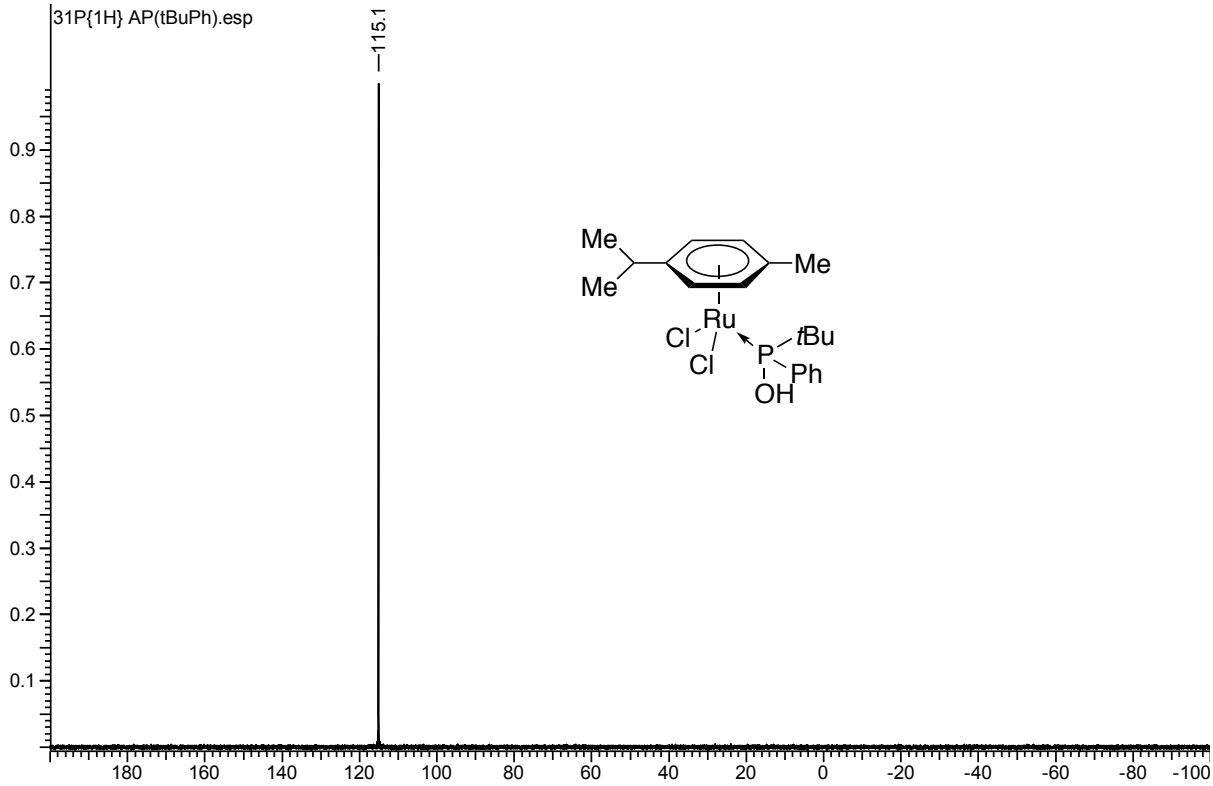

Figure 28. $^{31}P\{^{1}H\}$ NMR spectrum (162 MHz, $CDCl_3$) of [$RuCl_2$(η^6-*p*-cymene)(*t*-BuPhPOH)] **5l**

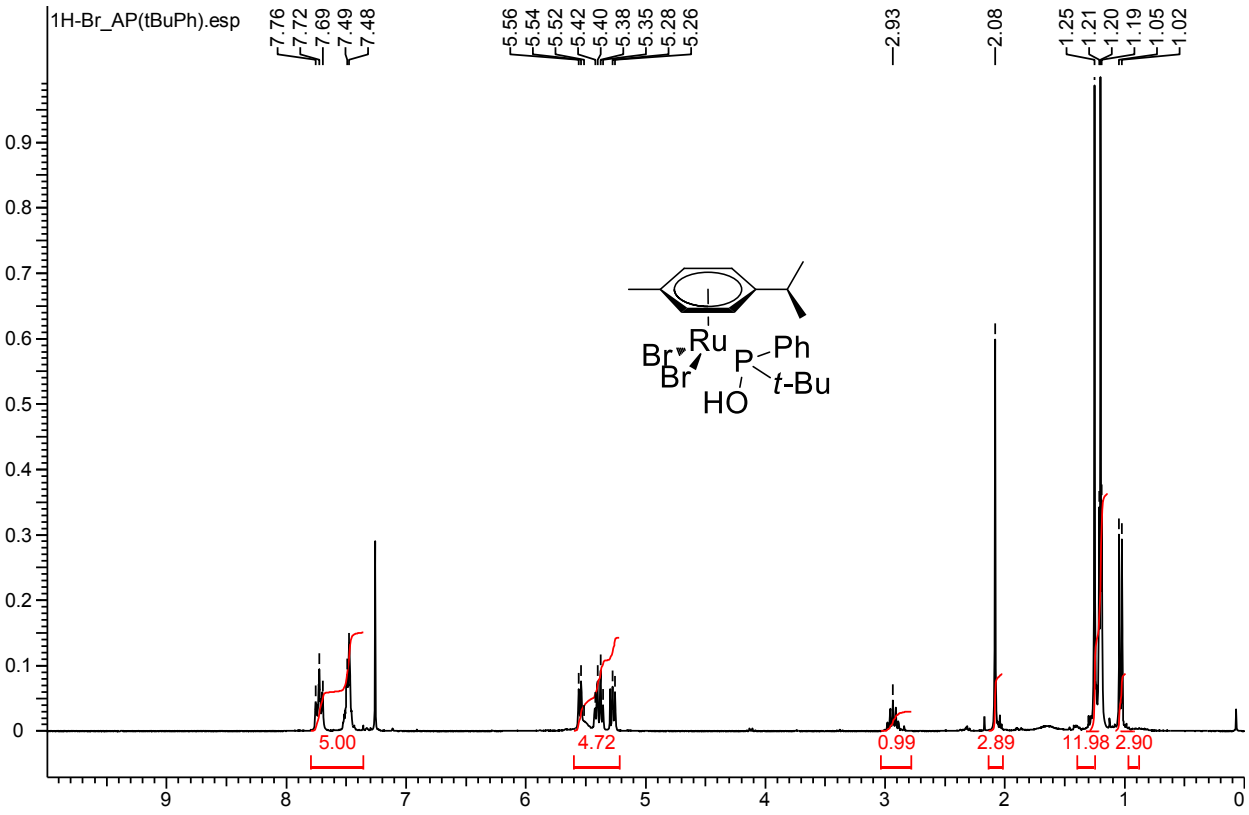

Figure 29. ^{1}H NMR spectrum (300 MHz, $CDCl_3$) of [$RuBr_2$(η^6-*p*-cymene)(*t*-BuPhPOH)] **6l**

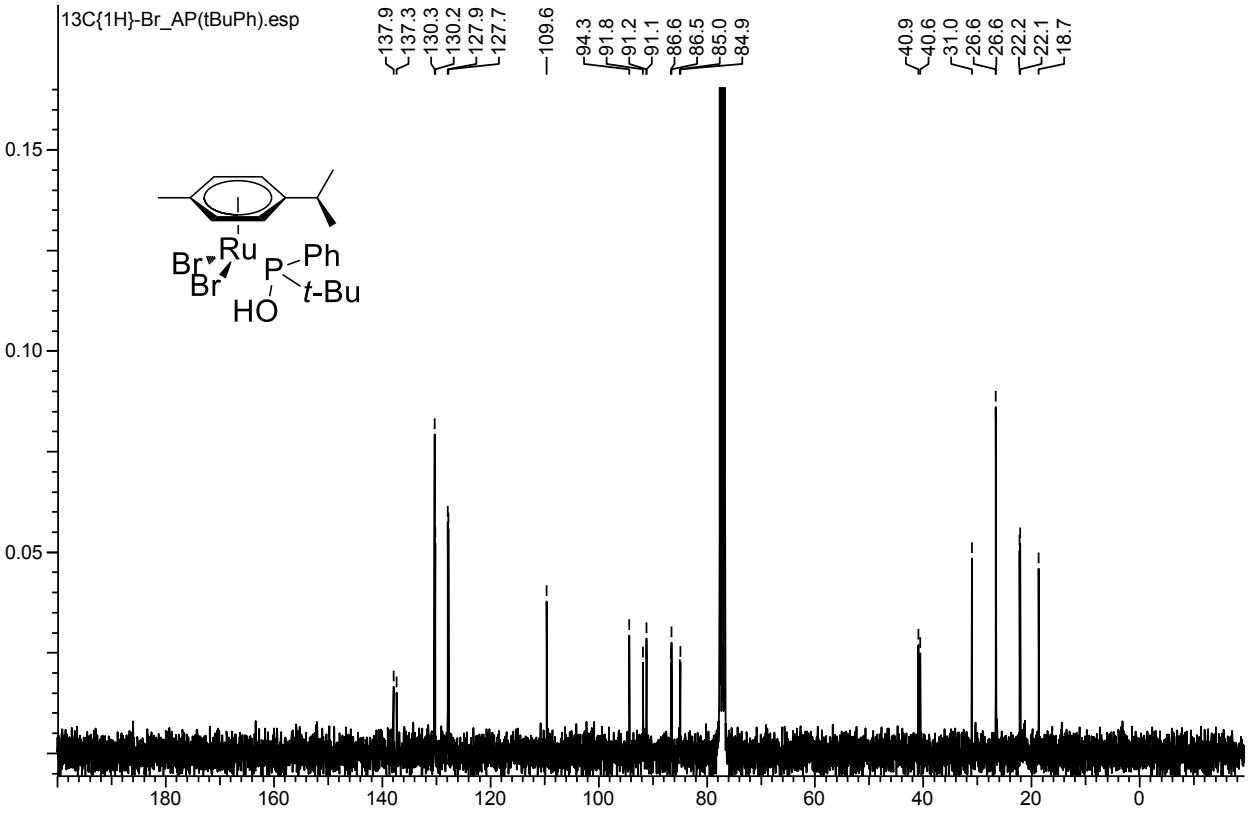

Figure 30. $^{13}C\{^{1}H\}$ NMR spectrum (75 MHz, $CDCl_3$) of [$RuBr_2$(η^6-*p*-cymene)(*t*-BuPhPOH)] **6l**

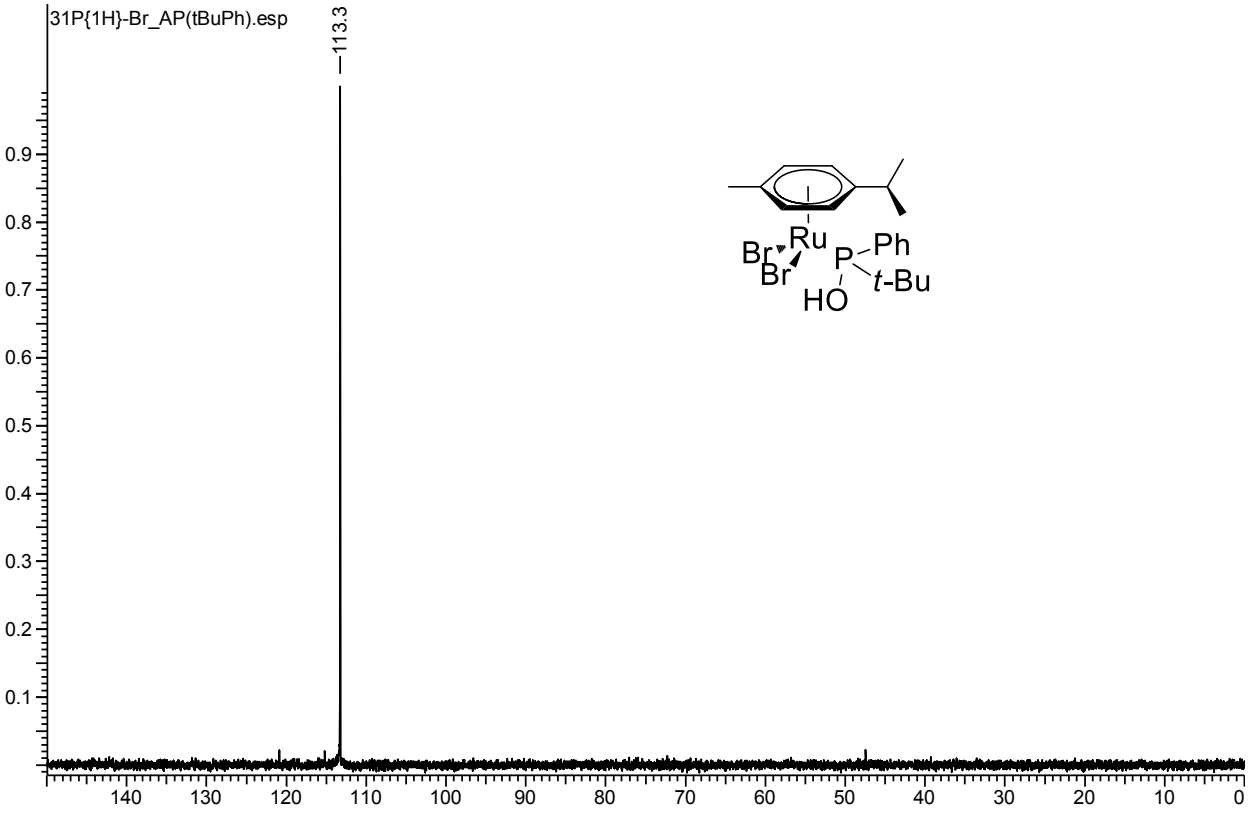

Figure 31. $^{31}P\{^{1}H\}$ NMR spectrum (121 MHz, $CDCl_3$) of [$RuBr_2(\eta^6$-*p*-cymene)(*t*-BuPhPOH)] **6l**

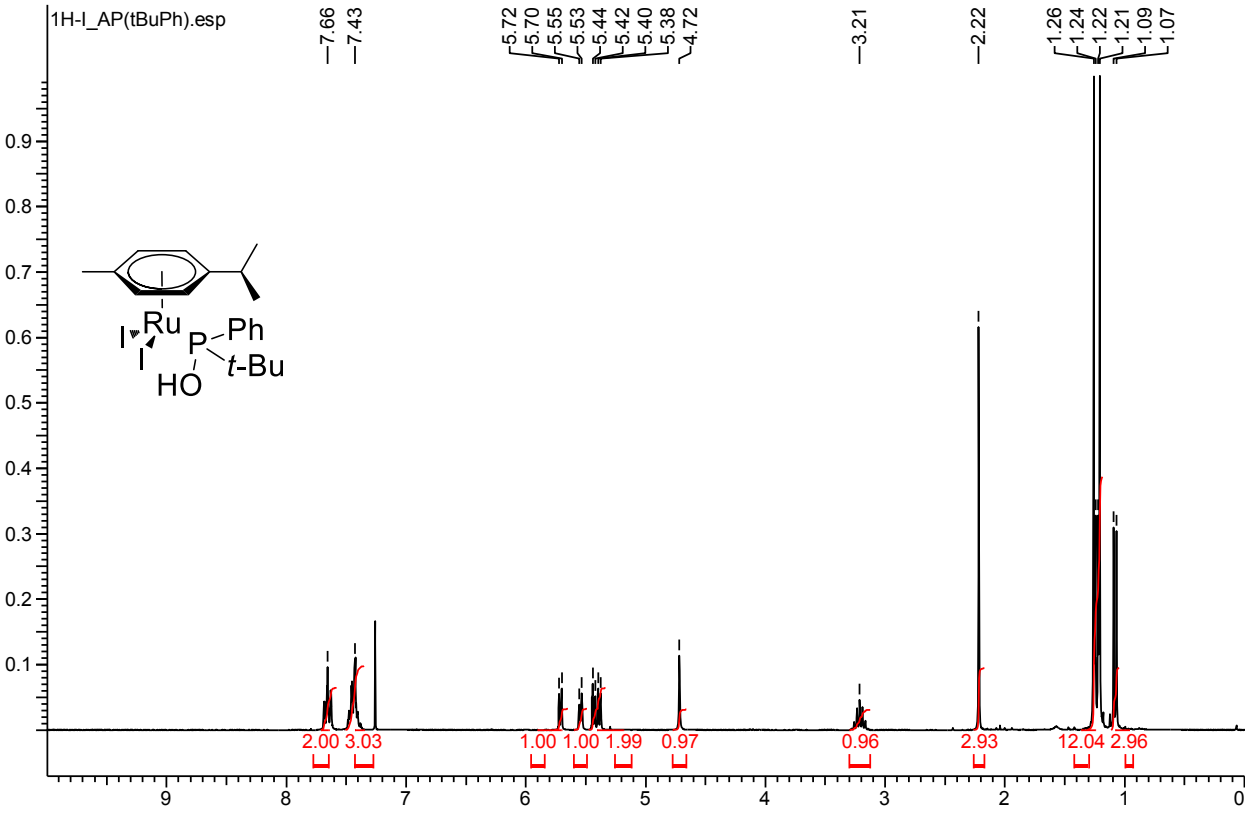

Figure 32. ^{1}H NMR spectrum (300 MHz, $CDCl_3$) of [$RuI_2(\eta^6$-*p*-cymene)(*t*-BuPhPOH)] **7l**

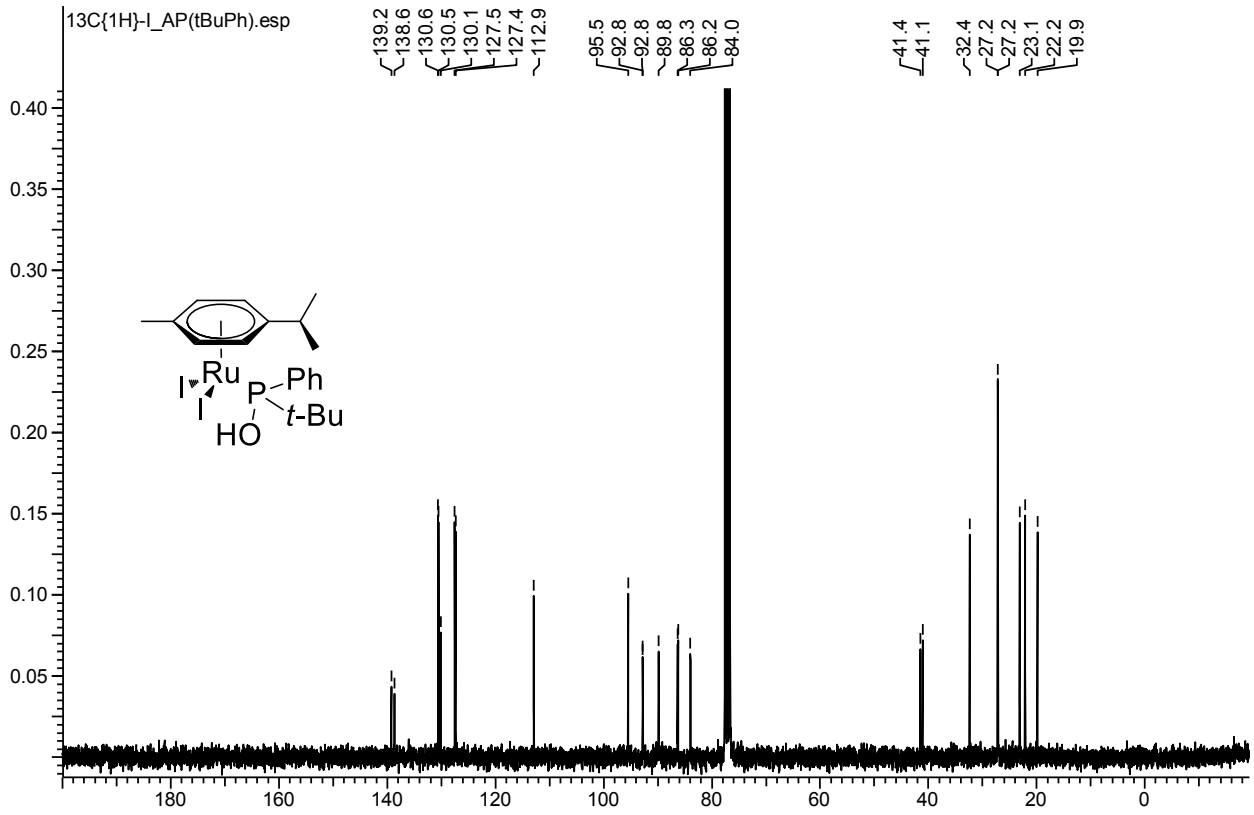

Figure 33. $^{13}C\{^{1}H\}$ NMR spectrum (75 MHz, $CDCl_3$) of [$RuI_2(\eta^6$-*p*-cymene)(*t*-BuPhPOH)] **7l**

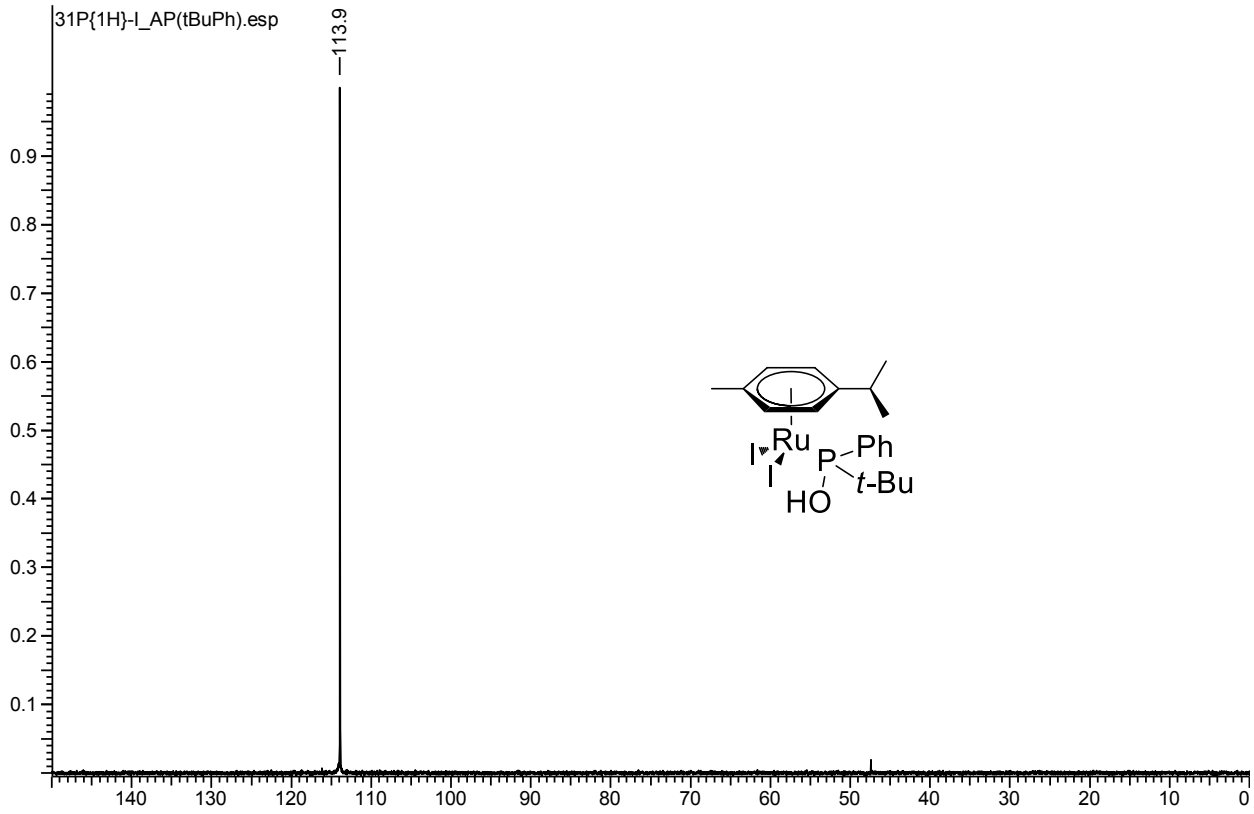

Figure 34. $^{31}P\{^{1}H\}$ NMR spectrum (121 MHz, $CDCl_3$) of [$RuI_2(\eta^6$-*p*-cymene)(*t*-BuPhPOH)] **7l**

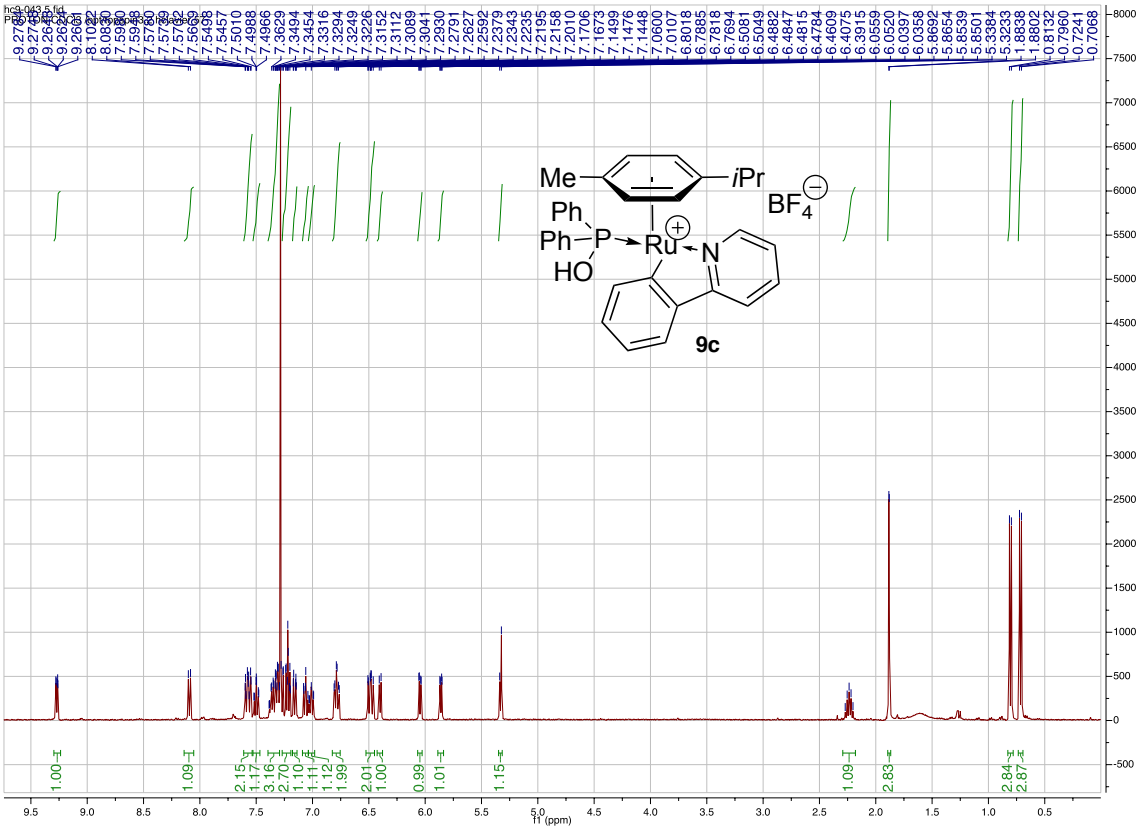

Figure 35. ^{1}H NMR spectrum (400 MHz, $CDCl_3$) of [Ru(η^6-*p*-cymene)(Ph_2POH)(2-phenylpyridine-κ^2-NC)BF_4] **9c**

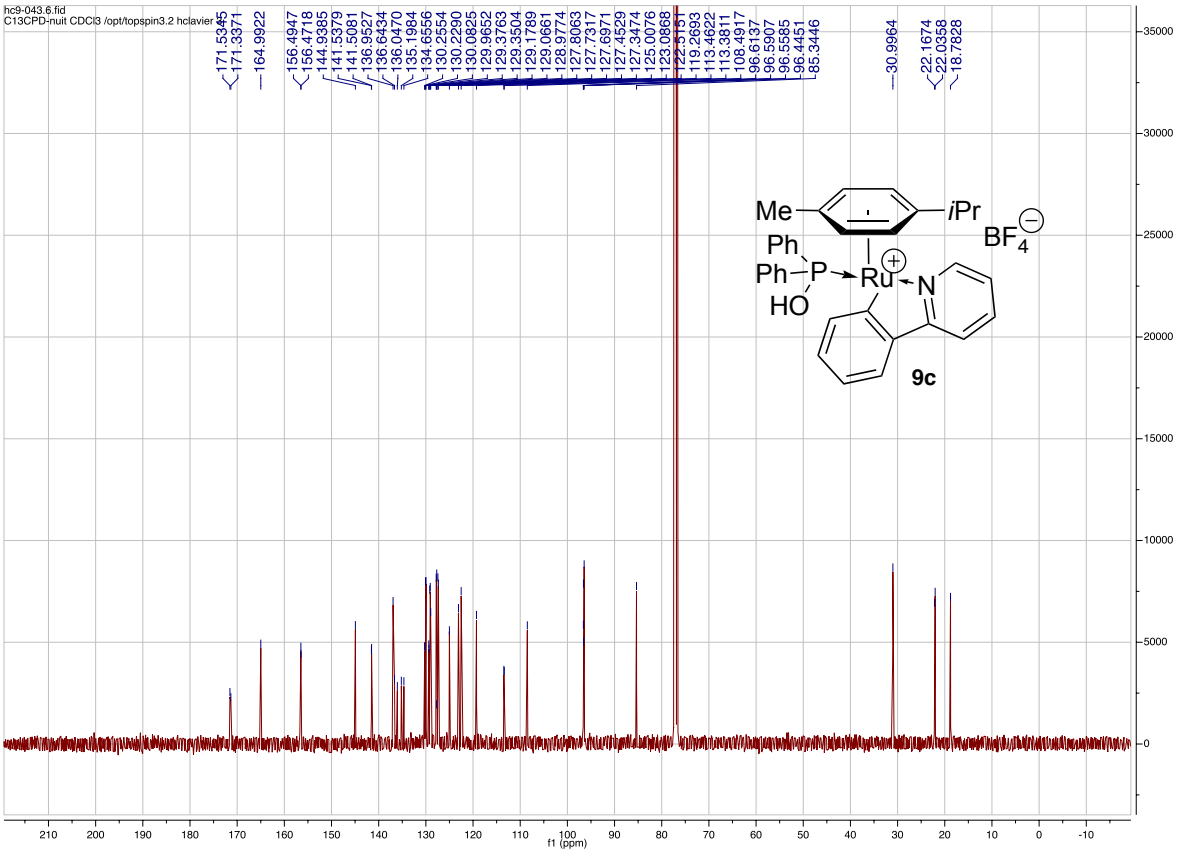

Figure 36. $^{13}C\{^{1}H\}$ NMR spectrum (100 MHz, $CDCl_3$) of [Ru(η^6-*p*-cymene)(Ph_2POH)(2-phenylpyridine-κ^2-NC)BF_4] **9c**

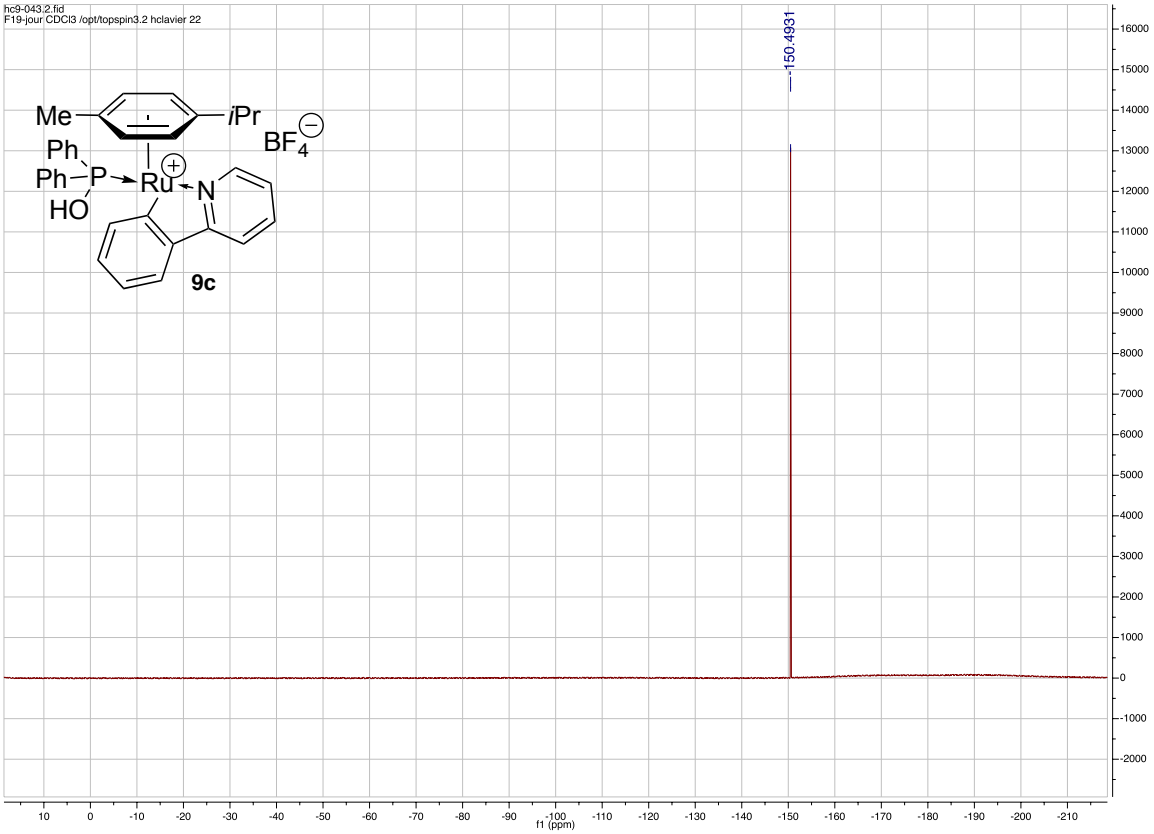

Figure 37. ^{19}F NMR spectrum (376 MHz, $CDCl_3$) of [Ru(η^6-*p*-cymene)(Ph_2POH)(2-phenylpyridine-κ^2-NC)BF_4] **9c**

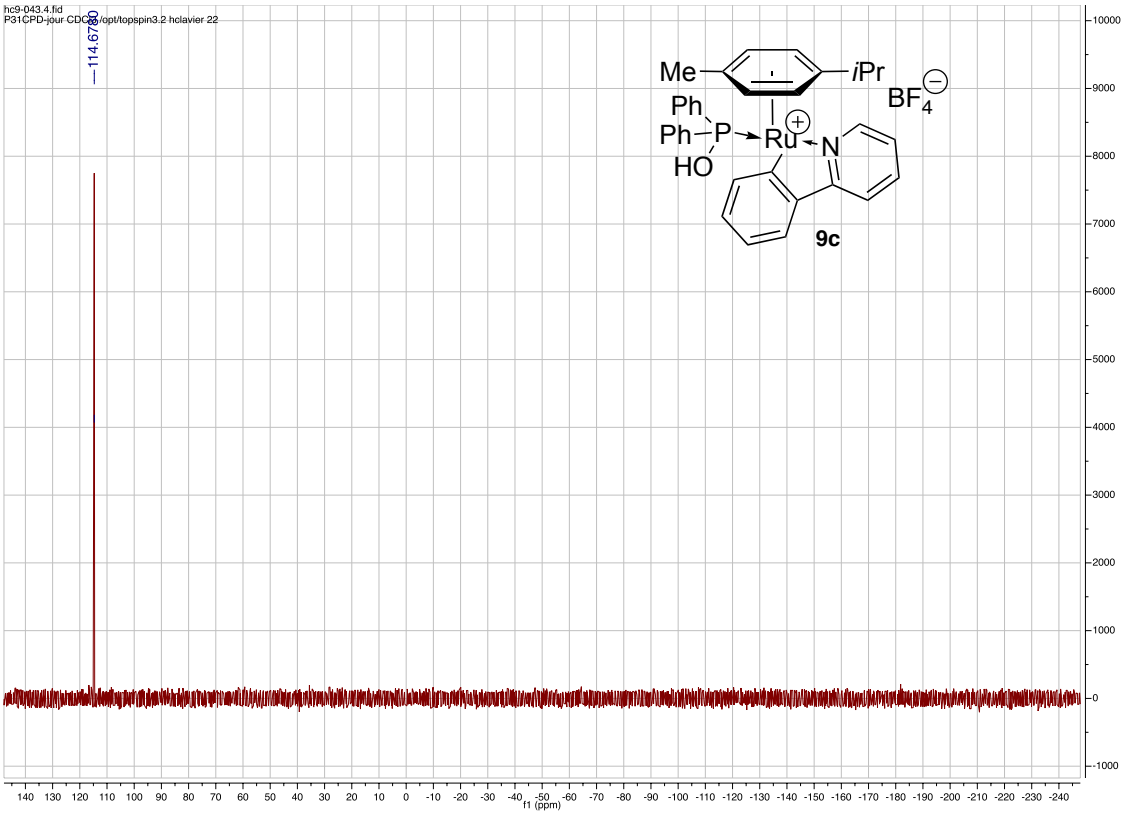

Figure 38. $^{31}P\{^1H\}$ NMR spectrum (162 MHz, $CDCl_3$) of [Ru(η^6-*p*-cymene)(Ph_2POH)(2-phenylpyridine-κ^2-NC)BF_4] **9c**